DOE/MC/31224 -- 5377
Distribution Category UC-132

Naturally Fractured Tight Gas Reservoir Detection Optimization

Quarterly Report
January 1 - March 31, 1996

Work Performed Under Contract No.: DE-AC21-94MC31124

For
U.S. Department of Energy
Office of Fossil Energy
Morgantown Energy Technology Center
P.O. Box 880
Morgantown, West Virginia 26507-0880

By
Coleman Research Corporation
5950 Lakehurst Drive
Orlando, Florida 32819-8343

Disclaimer

TABLE OF CONTENTS

1.0 3D P-WAVE ALTERNATE PROCESSING 3

1.1 3D P-Wave Interpretation 3

1.2 Comparisons of the E/W and N/S Azimuth Prestack Time Migrations 3

1.3 Structural Mapping of Horizons 3

1.4 AVOA Analysis 4

1.5 SAVI Analysis 4

2.0 DOWN HOLE 3C GEOPHONE ANALYSIS 5

2.1 Near Surface Variability in Shear Wave Velocity Anisotropy 5
2.1.1 Summary 5
2.1.2 Introduction 5
2.1.3 Field Procedure 5
2.1.4 Data Processing 7
2.1.5 Results 7

3.0 FRACTURE PATTERN ANALYSIS OF THE FORT UNION & WIND RIVER BASIN10

3.1 Theoretical Study 10

3.2 Basement study 11

3.3 Surface Studies 11
3.3.1 Air Photography 12
3.3.2 Regional Geologic Study 12
3.3.3 Field Mapping 12

3.4 Well Fracture Study 12

3.5 Production Information 13

4.0 3D-3C SEISMIC PROCESSING 15

5.0 TECHNOLOGY TRANSFER 17

6.0 REFERENCES 18

1.0 3D P-Wave Alternate Processing

Standard processing of the 37 square mile 3D was completed during this quarter. The final data volumes were shipped to the owner/operator for loading on their work station by Palantir and also shipped to Lynn, Inc. Also, all the amplitude variation with offset and azimuth volumes were shipped to the owner/operators work station for interpretation by Palantir. Limited offset stacks to 5,000 feet for the East/West and North/South volumes were produced from the final data in order to analyze the effects of fold on the data quality. The final processing sequence to be performed on the data was the SAVI (Semblance Analysis Volumes for Interpretation) routine. This procedure is similar to the coherency cube offered by Coherence Technology and represents the latest method for identifying faults in 3D seismic data. SAVI will be run on both the East/West and North/South volumes. Current interpretation status is described in further detail below.

1.1 3D P-Wave Interpretation

Interpretation of the 3D data began on both the owner/operators work station and on the Lynn, Inc., work station. Further descriptions of this work are given below.

1.2 Comparisons of the E/W and N/S Azimuth Prestack Time Migrations

An initial comparison was made by Lynn, Inc., of the E/W and N/S azimuth prestack time migrations under the area of the 3D-3C data acquisition. Significant travel time, amplitude and frequency anomalies were observed at the top of the Lower Fort Union and also throughout the Lower Fort Union and Lance Formations. One example of differences for in-line 70 is described below and can be seen in further detail in Figure 1.1a and 1.1b.

In-Line 70

On the shallow (0.5sec to 1.0sec) section just north of the 3C receiver grid, clear strong reflectors are present. The E/W near offset coverage is better shallow than the N/S coverage, but this does not appear to affect the data. At the top of Lower Fort Union (1.3sec to 1.5sec), the E/W data shows clear strong reflector character, whereas the N/S data have low amplitude, broken up reflectors. Within the Lower Fort Union (1.5sec to 2.0sec), poor signal to noise is evident in both the N/S and E/W sections. At the Lance (2.1sec to 3.0sec), a large travel time anomaly is observed with the E/W data showing an apparent syncline in time, and the N/S showing a flat reflector. This feature may represent a depth migration problem for future analysis.

1.3 Structural Mapping of Horizons

Palantir began by re-picking horizons for the Lower Fort Union using those originally picked by the owner/operator as seed horizons. Adjustments were then made for the difference in the East-West and North-South volumes. Two horizons were picked in the Lower Fort Union. A horizon was picked above the Lower Fort Union for the Waltman Shale to be used for normalization for interval calculations of the Lower Fort Union. The Waltman horizon was picked at Lynn, Inc., and the horizon has been imported into the owner/operator's work station for further calculations.

1.4 AVOA Analysis

Western Geophysical completed the AVO (amplitude variation with offset) gradient and intercept volumes on the DMO'd and prestack migrated gathers of the 3D volume for each azimuth in early March. These were then loaded onto the owner/operators work station for analysis by Palantir. The data horizons picked by the owner/operator were transferred to the new volumes and, after adjustments, were used as the horizons for the AVO analysis. Interval analysis was then performed using the IESX Computation Manager Software. The initial intervals analyzed were: the Lower Fort Union top plus 100msec; the Lower Fort Union top to base of Lower Fort Union; 25msec above the Lower Fort Union to 25msec below the Lower Fort Union. A comparison of these and some new intervals will be made at the beginning of the next quarter. The new intervals will correspond to the geological horizons picked by the owner/operator's geologists. For each of these horizons, interval AVO gradient and intercept calculations will be performed and compared to the gas production figures and the repeat formation tests conducted in the wells.

1.5 SAVI Analysis

Analysis of the N/S and E/W SAVI volumes will be made by transferring the top of Lower Fort Union pick time to the data and then flattening on this. Once flattened, time horizons will be made corresponding to the geologic horizons determined for the AVOA analysis. Interval semblance will then be created between the horizons and displayed as a series of maps. These will then be compared to the production figures for the discrete intervals.

IN-LINE 70: EAST/WI

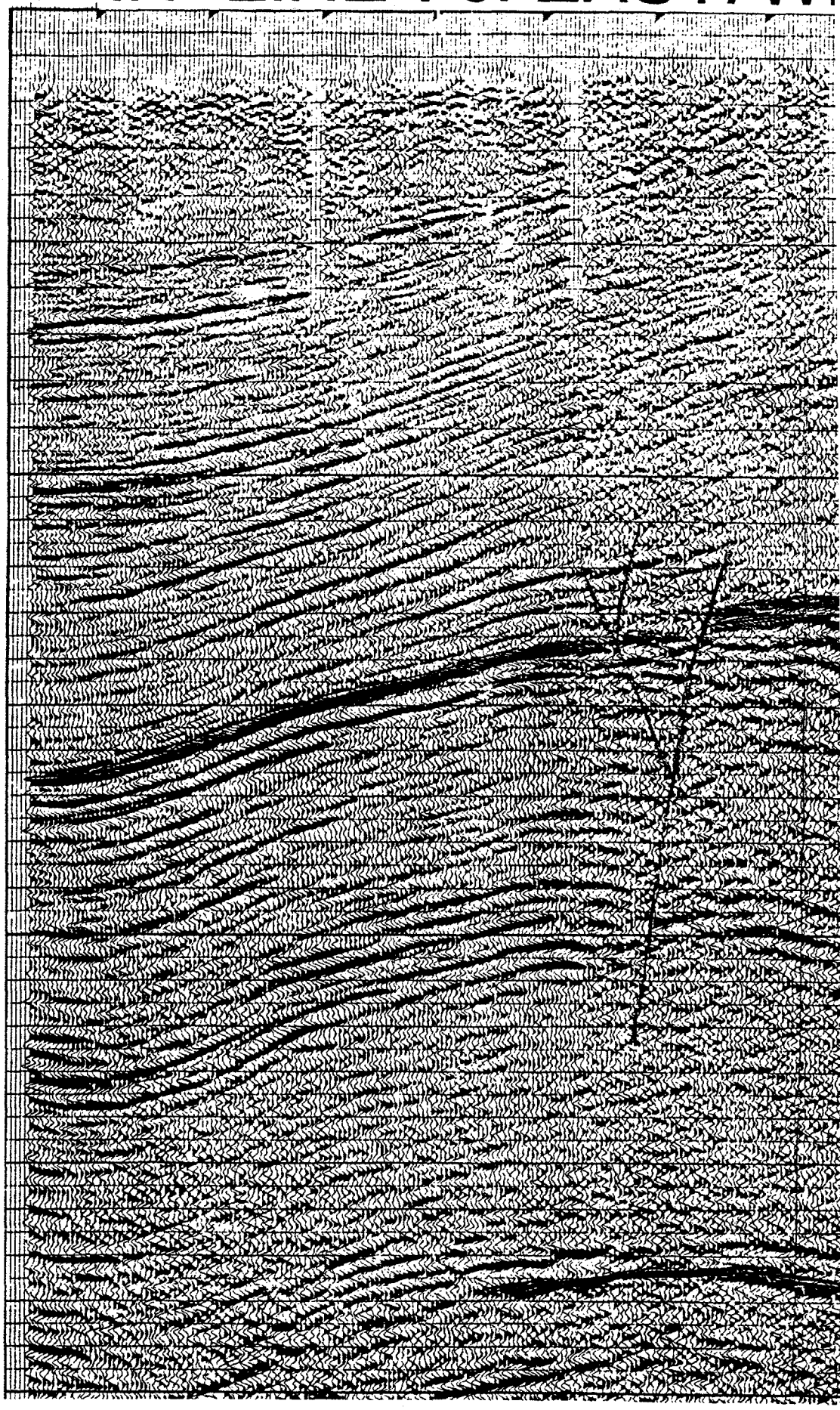

EST AZIMUTHS

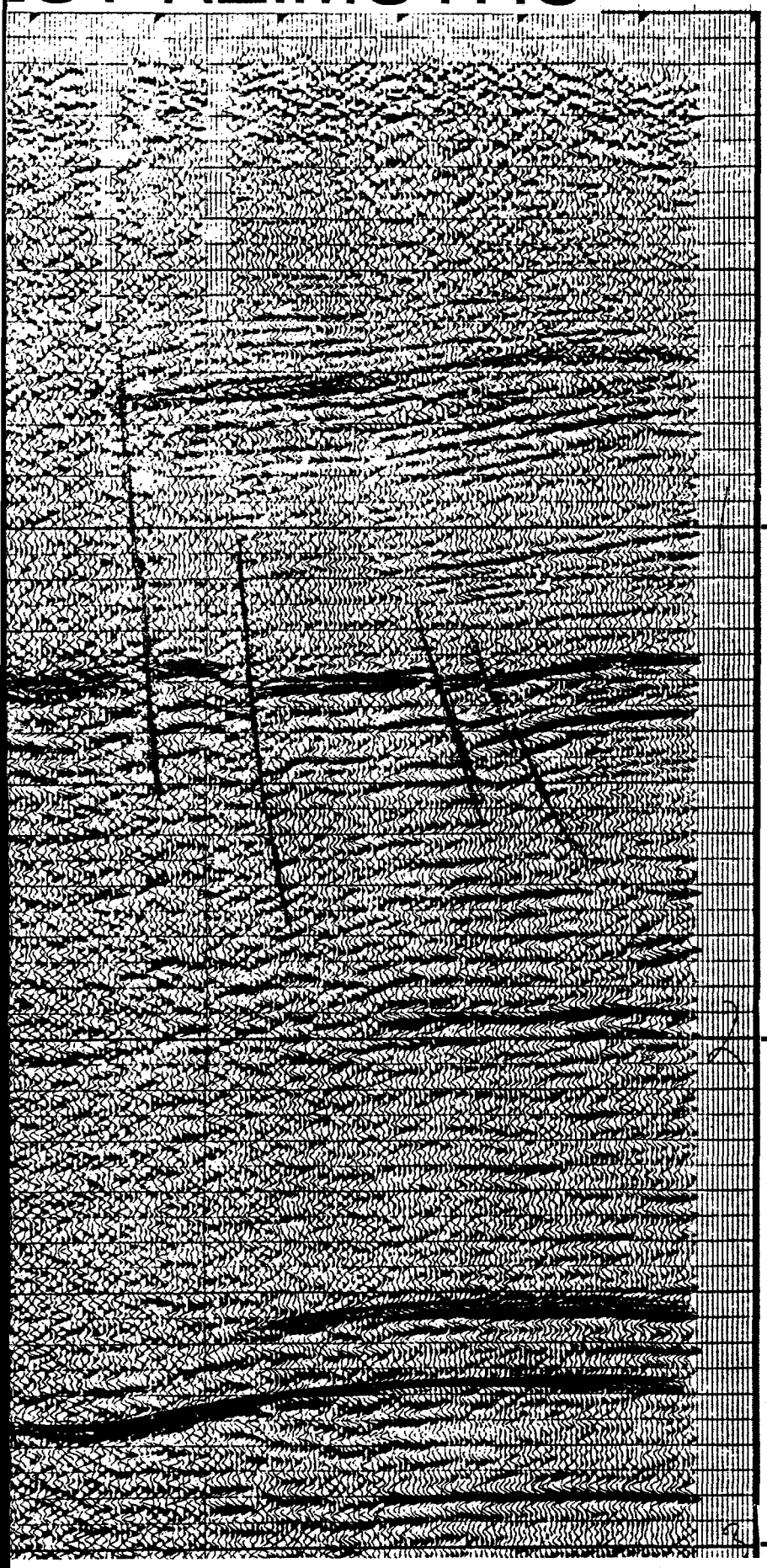

FIGURE 1-1A

IN-LINE 70: NORTH/SC

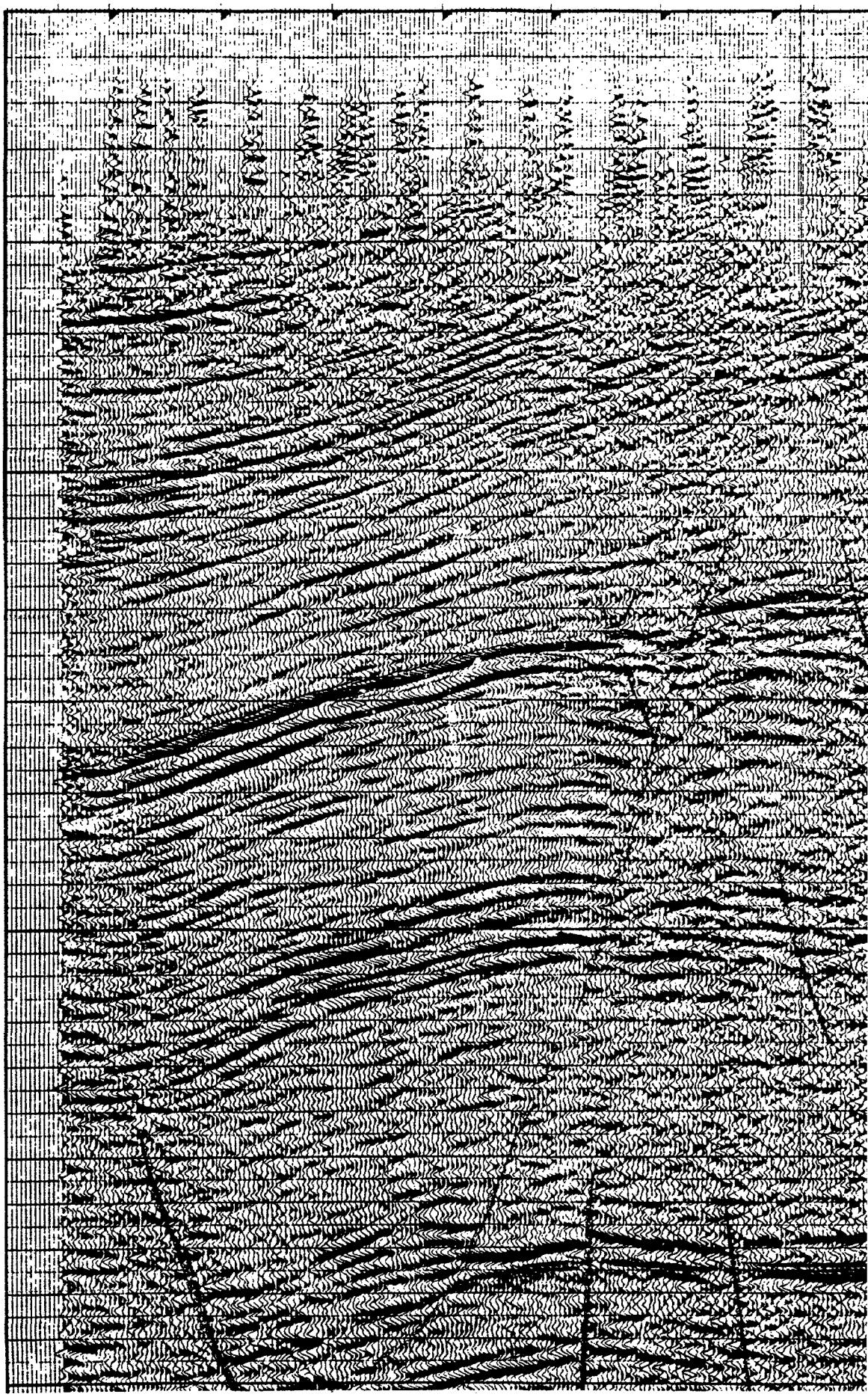

UTH AZIMUTHS

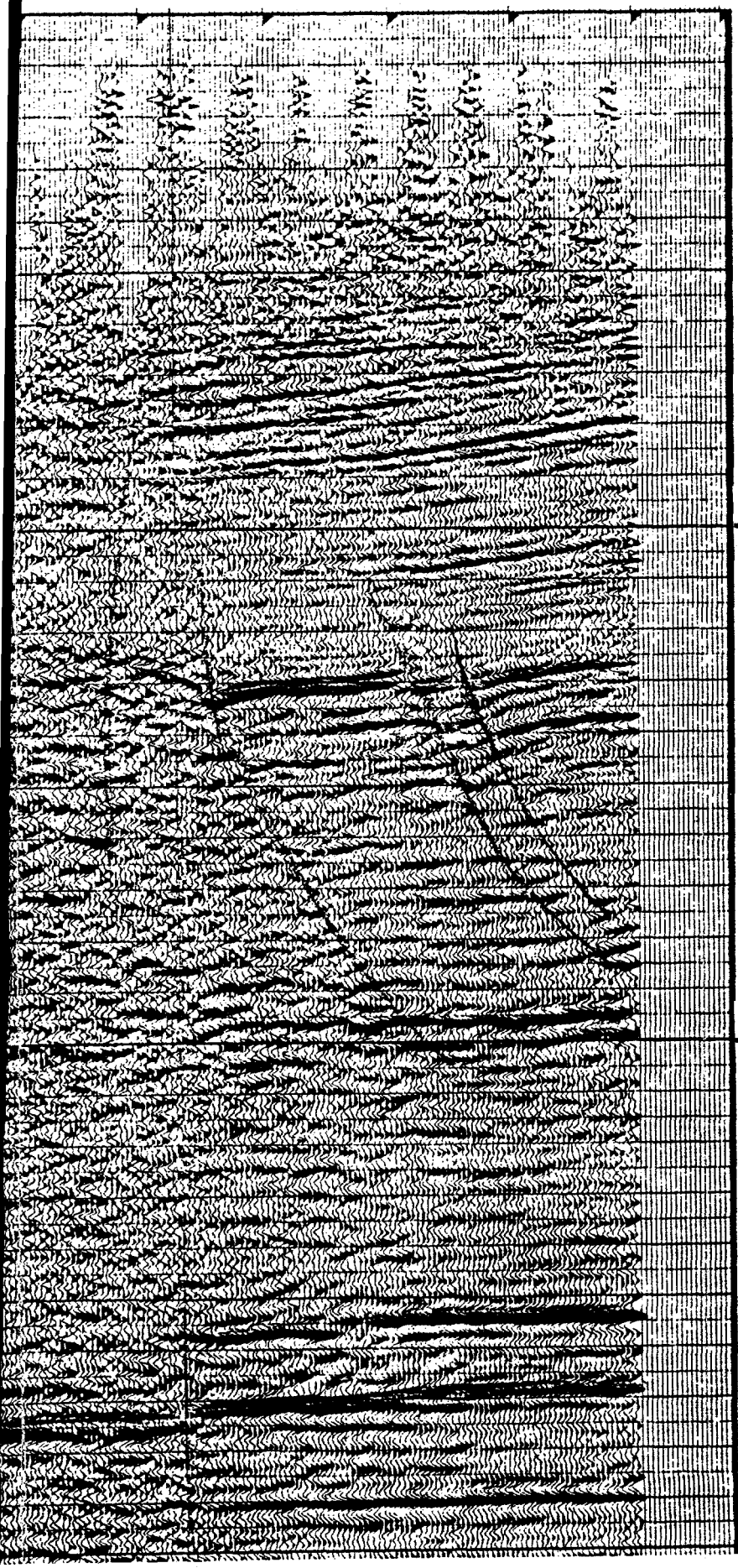

FIGURE 1-1B

2.0 Down Hole 3C Geophone Analysis

Before and during the acquisition of the 3D-3C seismic survey in the fall of 1995, a down hole, near surface analysis of seismic shear and compressional wave velocity was made. The purpose of this was to obtain velocities that could be used as a starting model for the static corrections that are necessary as part of the processing of the 3D-3C data and, also to determine if the near surface contained measurable seismic velocity that was similar to that recorded at depth. The results of the study have been written up for an expanded abstract to be presented at the 1996 Society of Exploration Geophysics Annual Convention to be held in Denver, Colorado, in October. The presentation is reproduced below.

2.1 Near Surface Variability in Shear Wave Velocity Anisotropy

2.1.1 Summary

The weathered layer has been shown to contain some of the greatest values of shear wave velocity anisotropy in the earth (Lynn, 1991; Crampin, 1990). The cause of the shear wave velocity anisotropy is most often either due to particle layering in unconsolidated sediments and sedimentary rocks, or due to aligned weaknesses commonly manifest as aligned open fractures. The aligned open fractures can be vertical and cross cut bedding in sedimentary rocks, or can be horizontal to sub-horizontal and are aligned with bedding. The purpose of this study was to measure the variation in properties associated with the vertical or sub-vertical fractures as these fractures often provide preferential pathways to fluid migration and can also influence recording of deeper seismic shear wave reflection data for oil and gas exploration.

2.1.2 Introduction

Near vertical fractures are typically formed during diagnetic processes, when a rock is subject to differential horizontal stress. After fractures have formed and opened, they are often infilled or partially infilled by material with different properties than the surrounding host rock. Later, during uplift and exposure from weathering, the fractures are accentuated being either more or less competent than the host rock. It has been shown that the presence of these aligned fractures, their density, and orientation can be measured using shear wave seismic techniques (For example, Crampin, 1985, Winterstein and Meadows, 1990, Macbeth, 1995).

This presentation describes a technique designed to measure the variability in near surface shear wave velocity anisotropy. Furthermore, the variation in shear wave velocity anisotropy and the orientation of the fast shear wave direction is interpreted in terms of vertical aligned fractures that display a preferred orientation.

2.1.3 Field Procedure

During the acquisition of a 3D-3C (three component recording) dynamite reflection seismic survey, a total of 30 three-component geophones were deployed in shotholes across the two square mile receiver patch. Typically, the explosive was loaded in a 60 foot deep hole with the down hole geophones attached below the charge. Seismic energy was then recorded from a surface impact source to the down hole 3C geophone. The geometry of the 3C borehole geophones is illustrated in Figure 2.1.

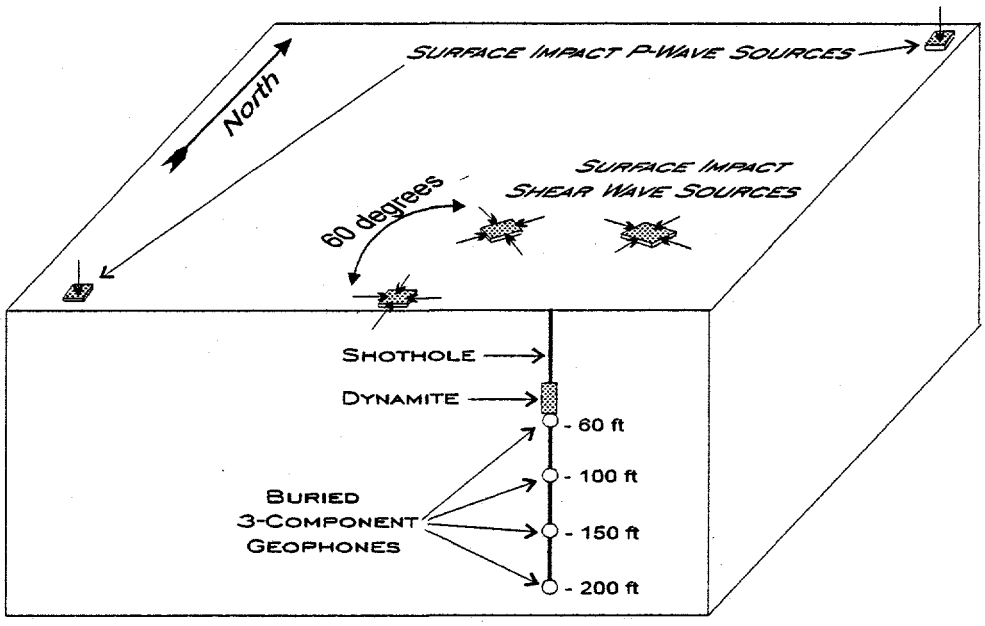

Figure 2.1. Acquisition geometry for collection of shear and compressional wave data for downhole receivers placed in shot holes.

The average depth over which the downhole impact surveys were made was 60 feet. At two locations in the field however, receivers were deployed at 60, 100, 150, and 200 feet. While the explosive detonation did destroy the downhole geophones, the method was more cost effective than drilling extra holes for the geophones. For 4D seismic acquisition, drilling of extra holes may be a more prudent long term method for measuring the near surface changes in shear wave velocity.

The down hole geophone assembly consisted of three single geophone elements arranged to be mutually orthogonal with two elements in the horizontal plane and one vertical. These were potted inside of an empty explosive sleeve, in order that the geophone assembly could be screwed onto the bottom of the explosive charge. No attempt was made to orient the geophones down hole, as it was intended to use a software rotation after recording the seismic energy to determine absolute azimuth.

For each buried phone location, three near offset shear and compressional wave source locations were surveyed. In addition, two far offset compressional wave source locations were used per hole for orienting the down hole assembly. The shear wave source consisted of a 60 lb steel plate coupled to the ground using six inch spikes. This source was struck on each end to create shear waves with their polarization direction perpendicular to the propagation direction. By striking the source on both ends, a reversal in shear energy was achieved which aids in identification of the shear arrivals. The source was oriented both radial and transverse to the hole approximately ten feet from the hole at each of the three locations. The compressional waves were created by striking the plate vertically.

The three source locations were compared to give an estimate of the error in this recording procedure. However, in future work only two locations should be sufficient as the measured velocity; and azimuth from all three positions gave results within five percent of each other.

2.1.4 Data Processing

The compressional wave velocity was measured from picking the arrival time on the vertical geophone element. A close correlation was obtained between the compressional arrival time from down hole recording and the uphole time recorded by the shooter when the explosive charge was fired (Figure 2.2).

The following sequence was used in the processing of the shear wave records. First, the data was sorted and geometry files written. A tool spin correction was applied using both the offset P-wave source locations. These results were compared for consistency in the corrections. The horizontal geophone elements were then rotated to be parallel and perpendicular to the shear wave source locations and a rotation analysis performed for the fast and slow shear waves following the method of Alford (1986). The resultant principal time series for the fast and slow shear waves were then used to re-create the original input data. If a close match was obtained with the original input data, the rotation was determined to be a success. From this, the azimuth of the fast shear wave was noted. The fast and slow shear wave time series were then cross correlated to obtain the time delay between fast and slow waves. The final output was a measure of the azimuth of fast shear wave, the time difference between fast and slow shear waves, and the magnitude of anisotropy in shear wave velocity.

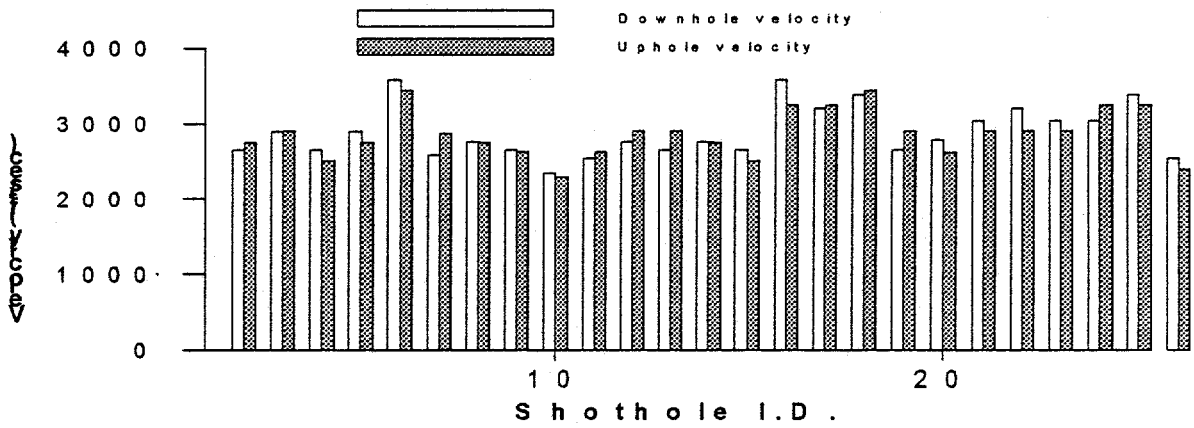

Figure 2.2. Compressional wave velocities calculated from surface sources and phones placed in the shotholes (Downhole), and from buried charges recorded by the uphole phones during the seismic survey (Uphole).

2.1.5 Results

The results for all 30 geophones are shown in a series of contour maps. In Figure 2.3, the VP/VS1 ratio is shown. Only at one place in the survey did the VP/VS1 ratio exceed three. Therefore, following the work of Sipos and Marshall (1995), it may be inferred that this is the only location which truly belongs to a weathered layer case. Therefore, at this location the P-wave static solutions cannot be used to construct shear wave static solutions in the absence of specific shear wave data. Thus, careful attention to static solutions and the S1/S2 ratio should be paid in this area. At all other locations, the P-wave static solutions could be used with the VP/VS1 ratio to model shear wave static solutions. Furthermore, the S1 static solution could be used to model the S2 solution.

Figure 2.4a illustrates the percent shear wave anisotropy and fast shear wave azimuth. The fast shear azimuth shows a consistent direction approximately East-West.

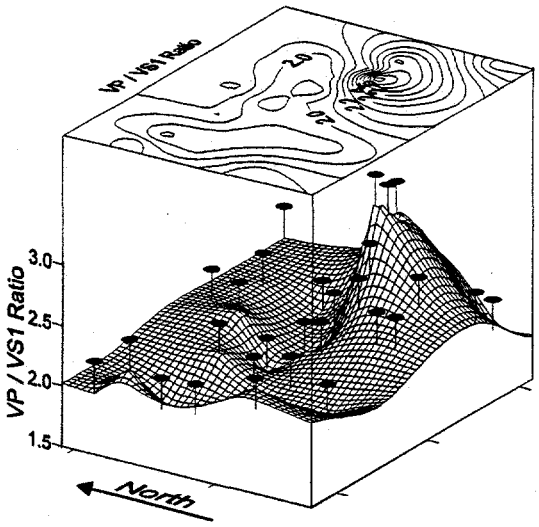

Figure 2.3. VP/VS1 ratio as measured by the buried geophone arrays. Black circles correspond to measurement locations.

This direction is plotted on a rose diagram in Figure 2.4b and is similar to that measured from air photography for faults, fractures, and linear geomorphic trends. The fast direction is parallel to the long axis of an open fracture with the slow direction perpendicular to this or across the open fractures. Thus, the fast and slow shear directions are interpreted to indicate a predominant weakness direction aligned approximately East-West in the surface rocks. The magnitude of shear wave anisotropy is a measure of the difference between fast and slow shear waves and is greatest in the northern half of the survey where values greater than ten percent are observed. For most deeper seismic studies in the U.S., background shear wave velocity anisotropy is recorded at four percent or less. Therefore, the values of anisotropy recorded here are interpreted to be anomalously high. Crampin (1994) has indicated that values of shear wave velocity anisotropy over eight to ten percent represent a state of competency in the rock mass, where fracturing is so severe that a breakdown in shear strength occurs and enhanced permeability results. Thus, vertical hydraulic conductivity is also greater at this location. This has implications for engineering, hydrogeologic, and environmental assessment of the site.

It is also worth noting here that the location that contained the problem area for seismic static solutions is not the area that most concern should be paid for the environmental and engineering surveys. Nonetheless, the technique described here simultaneously addresses both problem areas. The variation in shear wave velocity anisotropy across the survey area is significant and indicates the potential for rapid variations in similar geologic settings.

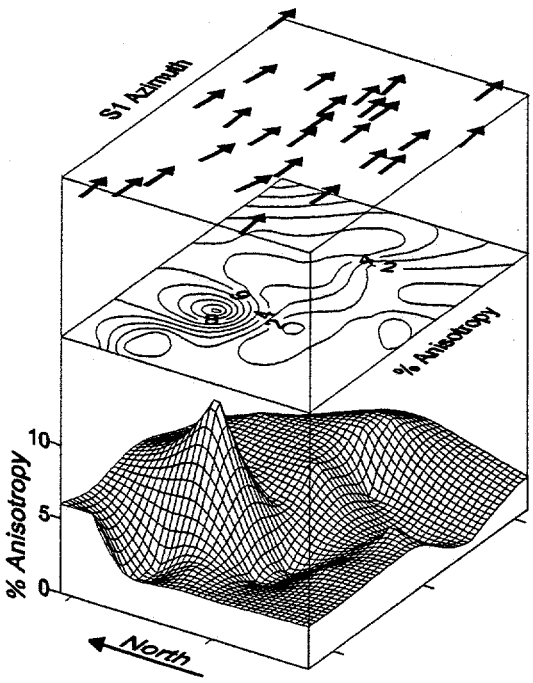

Figure 2.4a. Percent shear wave anisotropy and azimuth of the fast shear wave. Azimuth arrows correspond to measurement locations.

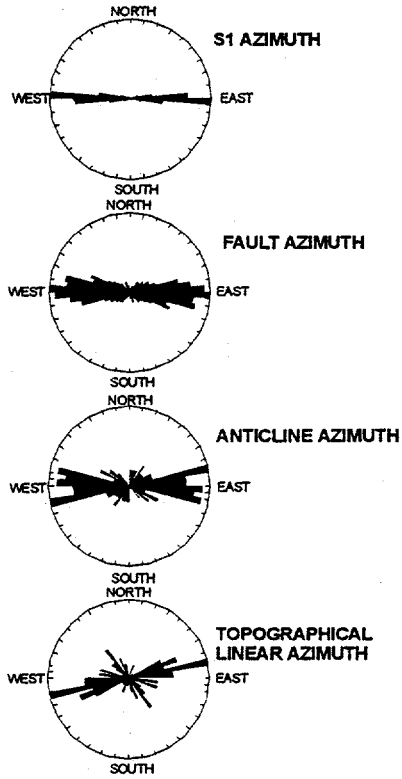

Figure 2.4b. Rose diagrams generated from fast shear wave azimuth, local fault azimuth, anticline azimuths, and topographical azimuths.

On observing this variability the question remains whether closer sampling would have identified even greater variation in shear wave velocity anisotropy and if these near surface lateral variations are also seen at depth. These issues will be the focus of the next phase of investigation.

3.0 Fracture Pattern Analysis of the Fort Union & Wind River Basin

The focus of this research project is to identify zones of naturally highly-fractured rock that produce significant volumes of gas. Much of the natural fracturing in Rocky Mountain basins, such as the Wind River Basin, was imparted to the rocks during Laramide age deformation. In particular, towards the end of the Cretaceous, while the Colorado Plateau was colliding with the North American Craton in a North-East direction, a compressional regime was set up in association with strike slip tectonics to create areas of uplift and massive thrusting and folding separated by broad deep basins. In the Wind River Basin, Wyoming, a large thrust cored anticline contains the tight, but naturally fractured sands of the Lower Fort Union Formation. These sands are the target of the DOE study. The process of the collision between the Colorado Plateau and the North American Craton produced fracturing patterns in many Rocky Mountain basins that are both predictable and can be mapped in the field. A knowledge of the general trend of fracturing across a region is important when designing and executing seismic programs that aim to identify the most productive zones of open, gas-filled fractures .

Four types of study have been undertaken to identify the most likely trend of the open fractures in the Wind River Basin and, in particular, in the Fort Union Formation; namely, a theoretical study, basement analysis, surface study, and borehole investigation. These are each described in further detail below.

3.1 Theoretical Study

Indenter theory, developed in metallurgy, shows that when a rigid die begins to penetrate a plastic solid, slip lines are set up along which left- and right- lateral shears subsequently develop. A major left-lateral shear develops from the left corner at 45° to the indenter front, and a similar right-lateral shear develops from the right corner. Other shears develop parallel to the major corner shears within the triangle, outside the triangle, radial shears develop from the corners. Molnar and Tapponier (1975) used slip-line theory to analyze the tectonics created by the indentation of India into Asia. Their method is followed here for the Colorado Plateau-North American Craton collision. Tapponier and Molnar (1976) expanded the slip-line theory, and Tapponier et al. (1982, 1986) used physical models to verify the results. Slip-line theory was used by Scheevel (1983) to analyze Rocky Mountain Foreland deformation, but with this study the emphasis was on vertical movement created by horizontal compression, not lateral movement. Applying slip-line theory to the Colorado Plateau-Foreland boundary, it is noted that the major right-lateral shear, which, conceptually, should run north from the southeast corner, is coincident with the San Luis Valley-Arkansas Valley trend in Colorado. The left-lateral shear which should run east from the northwest corner is coincident with the Duchesne fault system. The two fault systems intersect in North Park, Colorado. Although these two trends are the major faults in this scenario, strike-slip faults develop parallel to slip-lines along the Front Range of the Rockies on the east. On the west, the Wasatch Front north of the left indenter corner follows a slip-line. Strictly speaking, the slip-lines exist only at the initiation of indentation, once fracturing begins, secondary faulting and block rotation take place destroying the symmetrical pattern. Thus, to understand how the crustal tectonics may have developed, one must understand how rocks fracture under compression or shear couple in order to integrate the known faults of the region into this system of large-scale shears.

Sales (1968), Stone (1969) ,and Wise (1963) have proposed large-scale shearing and strike-slip faulting in the Rocky Mountain Foreland and their ideas are further extend here by examining the strike-slip fault systems so created. An excellent review of strike-slip faulting and the associated secondary structures, such as basins, uplifts, and thrusts can be found in Sylvester (1988). One of the conclusions which may be drawn, is that in a strike-slip fault system created either by compression, or by a couple, the rocks fracture systematically and that the fractures are scale-invariant. This phenomenon has been demonstrated by field mapping (e.g., Tchalenko, 1970; Tchalenko and Ambraseys, 1971), and by laboratory studies (e.g., Bartlett et al., 1981; Wilcox et al., 1973). The terminology used here was defined by Bartlett et al. (1981) who identified Y as the principal shear direction, and R and P as the synthetic shears disposed at 15° on either side of the Y direction. R is often called the Riedel shear; R′, the antithetic Riedel shear; and X, the other antithetic shear are disposed at 75° to the Y direction. These shears usually display oblique movement. Thrust and reverse faults develop perpendicular to the compression direction. Tension faults, T, develop parallel to the compression direction. Based on modeling studies, the fractures which are most likely to remain open while still in the compression regime are those with oblique movement: R′, X, and T fractures (e.g., Wilcox, et al, 1973). However, if compression is followed by subsequent tectonic activities that may include uplift of basins, unloading due to erosion and relaxation or extension, then other fracture orientations within the subsets defined by initial compression may be the preferentially open fractures today. Such periods of uplift are known to be the case in the Wind River Basin. Predicting the open fracture direction is one of the key focuses of the seismic program, where the predictions will be compared with the local gas production figures. The dominance of a preferred open fracture direction gives these type of gas reservoirs their antisotropic permeability. Evidence for asymmetric or anisotropic production is given later. In addition to lateral movement, strike-slip fault systems create paired uplifts and basins which often have 30,000 feet of relative vertical displacement (Crowell, 1974). The Wind River basin/South Owl Creek mountains represents such a pair.

3.2 Basement study

It has been shown in other studies, for example the DOE funded project in the Rulison Field, Colorado, that basement control on fracturing and faulting is extremely important in many fields for production of gas from fracture controlled reservoirs. In this project, the basement was analyzed using the regional magnetics and gravity. Figure 3.1a and 3.1b shows the results of both these regional studies with the outline of the Wind River Basin highlighted. On both maps, strong linear trends can be seen. These linear features also fall into the categories predicted by the theoretical treatment made by Bartlett et al (1981). This information is shown on the rose diagrams in both figures.

3.3 Surface Studies

Surface studies fall into a number of subcategories at various different scales from macro feature analysis using air photography to regional analysis using ground truth data from field outcrops.

3.3.1 Air Photography

A regional air photography study was paid for by the owner/operator of the Wind River field. This information was then reviewed for lineament analysis. Four categories of linear feature were identified namely:

- Faults - These are subdivided into features that are identified as faults with obvious displacement, probable faults, and inferred faults where no displacement is determined.
- Distinct Topographic Linear - more than half a mile in length.
- Visible fractures - to include drainages, vegetation, and topographic linear features on a small scale (less than half a mile in length).
- Anticlines, Synclines, or Monoclines - with sense of feature marked where apparent.

The results of this survey have been plotted using rose diagrams in Figure 3.2. These all show a distinct East-West component apart from the class of visible fractures which show a trend of linears Northwest-Southeast and Northeast-Southwest. These directions fall into orientations that are parallel and perpendicular to the original compression direction for the Colorado Plateau indenting the North American Craton (see sections 3.1 and 3,3,2). The Northwest-Southeast set, initially under compression by the collision, is perpendicular to the maximum horizontal compressive stress during the Laramide deformation. Thus, these fractures should be preferentially closed if the stress situation has been preserved to the present data, i.e. the basin is currently under a compressive stress regime. However, as the Lower Fort Union is thought to be currently under extension due to uplift and relaxation, this set could today be open or partially open.

3.3.2 Regional Geologic Study

The direction of major faulting was taken from the USGS regional geologic maps of Wyoming and the Wind River Basin and is shown in Figure 3.3 together with an interpretation based on the theoretical work of Bartlett et al (1981). The dominant direction of linear features is once again an East-West one (along the Y direction of the theoretical study). This direction is explained by a Northeast compression direction and a left lateral shear component.

3.3.3 Field Mapping

During the 1996 summer field mapping season, the outcrops of the Fort Union in the Wind River Basin, will be mapped to record any relationships between the fracturing patterns (direction, density, clustering) and the lithology. If relations exist and the lithology can be unitized in outcrop, then the well information will be studied to ascertain if the fracture relations can be predicted using the lithology in the producing field.

3.4 Well Fracture Study

Five wells across the field area have had various fracture analysis tools deployed in them through the Fort Union. In four wells, the Schlumberger Formation Microscanner Image log was run. This tool is an electrical resistivity device that measures the difference in electrical properties between a rock and a fracture. The fractures are imaged if they are either open or filled with a material with different electrical property than the host rock. The tool is capable of imaging the fractures and from computer analysis, the strike and dip of the fractures can be measured. Figures 3.4 and 3.5 show examples of the data output and interpretation. The results of the fracture analysis are shown in Figure 3.6 in a series of rose diagrams for depths from 5,343 feet

below KB to 9,200 feet below KB. Once again, an East-West trend is dominant. The results for all four FMI analyses are shown in Figure 3.7.

In one well in the field, the Western Atlas CIBL (Circumfrential Borehole Imaging Log) tool was deployed. CIBL is an acoustic borehole imaging tool that uses rotating transducers to scan the borehole wall with transmitted acoustic pulses. The tool measures the travel time and amplitude of acoustic signals reflected by the borehole wall. Variations in lithology and physical rock features, such as fracturing, are imaged with the tool. The analysis of imaged data also produces a measurement of fracture strike and azimuth. The results for the CIBL analysis are displayed in Figure 3.8 and show a dominant trend south of East-West for depths between 7,100 feet and 9,800 feet rotating to East-West below 13,000 feet. The results for all depths are plotted together with those for the FMI on Figure 3.7. The location of each of these wells is along the axial crest of the structure.

Great care must be taken with the interpretation of these results and particular attention should be paid to the dominant fracture trend in any well at specific depths with regard to the local structure. For example, it has been shown that fracture trends can rotate from the regional patterns close to major faults. When the final structure and fault maps are produced from the horizons within the Fort Union, these well data will be further reviewed.

3.5 Production Information

In Figures 3.9a and 3.9b, the production numbers for Lower Fort Union wells are displayed. On Figure 3.9a, the production for the six months prior to the acquisition of the 3D survey is contoured. In Figure 3.9b, the initial six months production is given. For the initial six month production, an attempt was made to normalize the production to the actual number of days where the well was producing during the first six months. From both figures, it can be seen that the highest production is centered around the crest of the Lower Fort Union Formation.

The graph in Figure 3.10 shows the results of conducting Repeat Formation (pressure) Tests (RFTs) in four wells during the drilling process (see Figure 3.9 for the location of the wells). The RFTs are conducted subsequent to drilling and consist of making formation pressure tests in the side walls of the well at discrete intervals. The results are plotted as pressures with depth. The solid line on the graph represents the predicted virgin or undepleted formation pressure. Also shown in the graph is the pressure at two other wells in the field (D6 and D18) at the time the RFTs were conducted. Most of the RFTs scatter close to the undepleted predicted line with only partial drainage throughout most of the section. However, between 6,800 feet and 7,500 feet partial depletion is seen in the two wells that are approximately West and East of D6 and D18 and adequate depletion is seen in the wells that are Northwest and Southeast of D6 and D18. One possible explanation of this is preferential communication in a Northwest-Southeast direction. This direction was seen in some of the air photography work and is perpendicular to the Laramide compression direction. Therefore the hypothesis of subsequent extension or relaxation thus opening this fracture set (as proposed in section 3.3.1) is supported. However, to fully appreciate the implications of the well communication, each well must be located with respect to the fault system as compartmentalization issues must be addressed. This will be done when the final structural maps are avaliable.

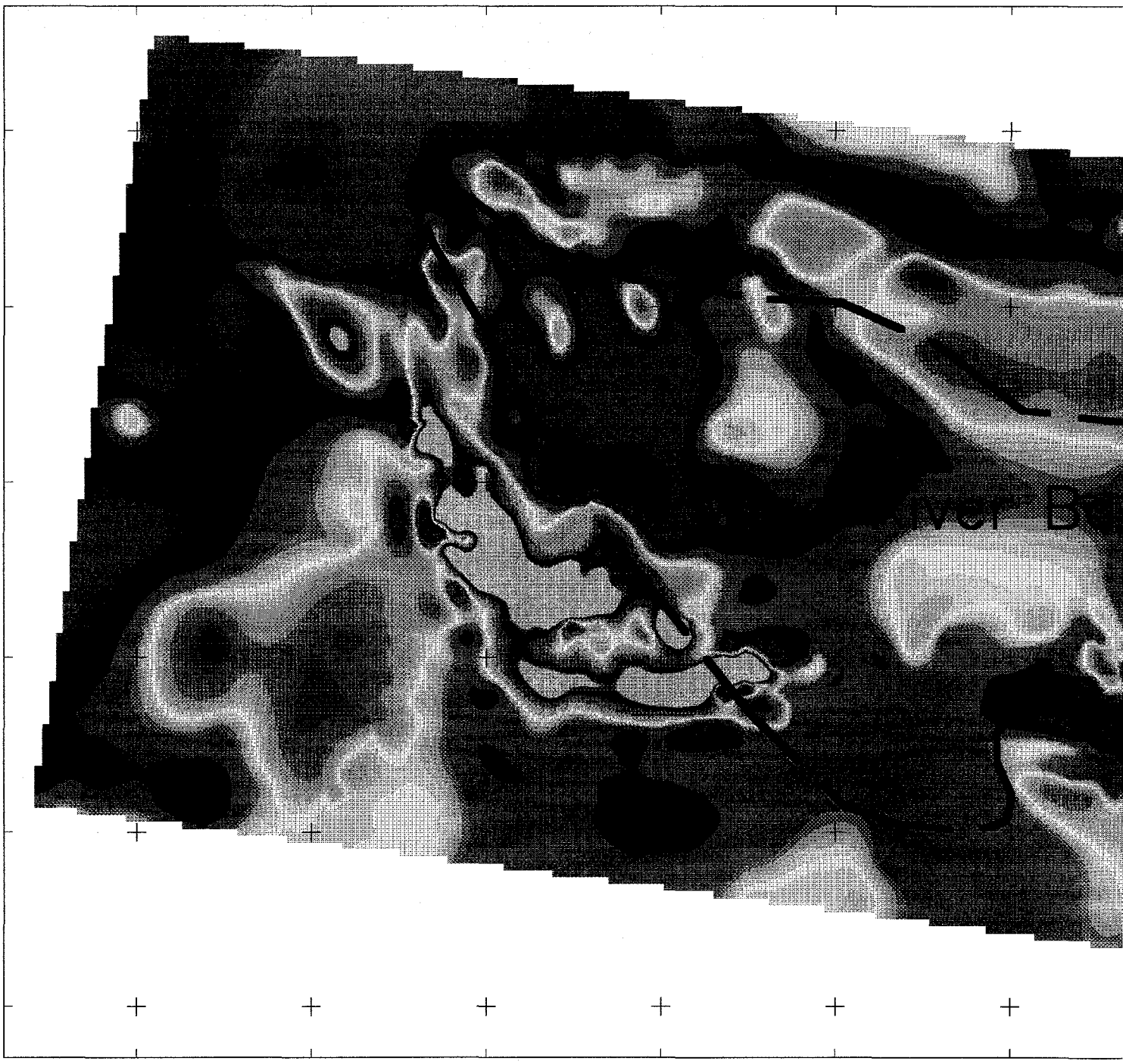

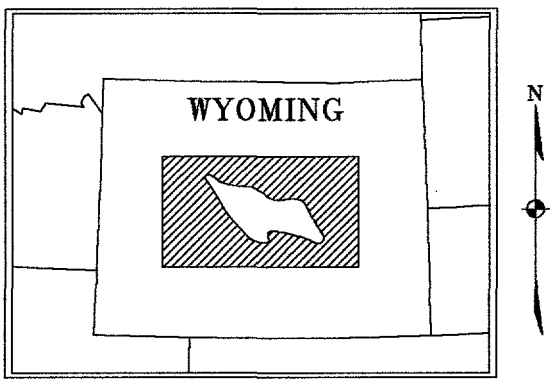

WIND RIVER BASIN
LOCATION MAP

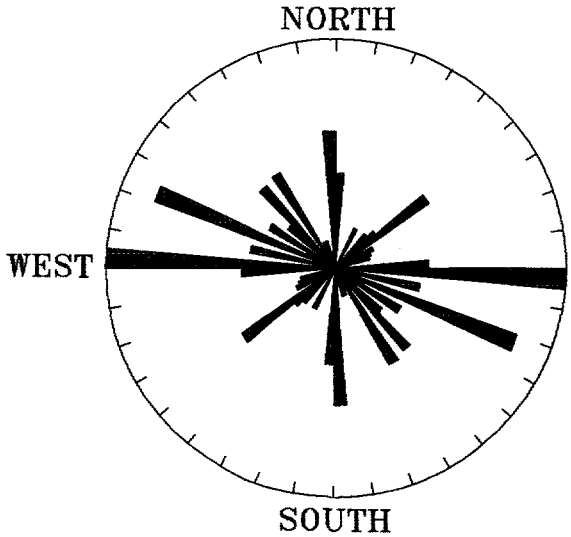

MAGMASK.GRD
\PROJECTS\MAD\QTR4-96\MAGFNL.PLT

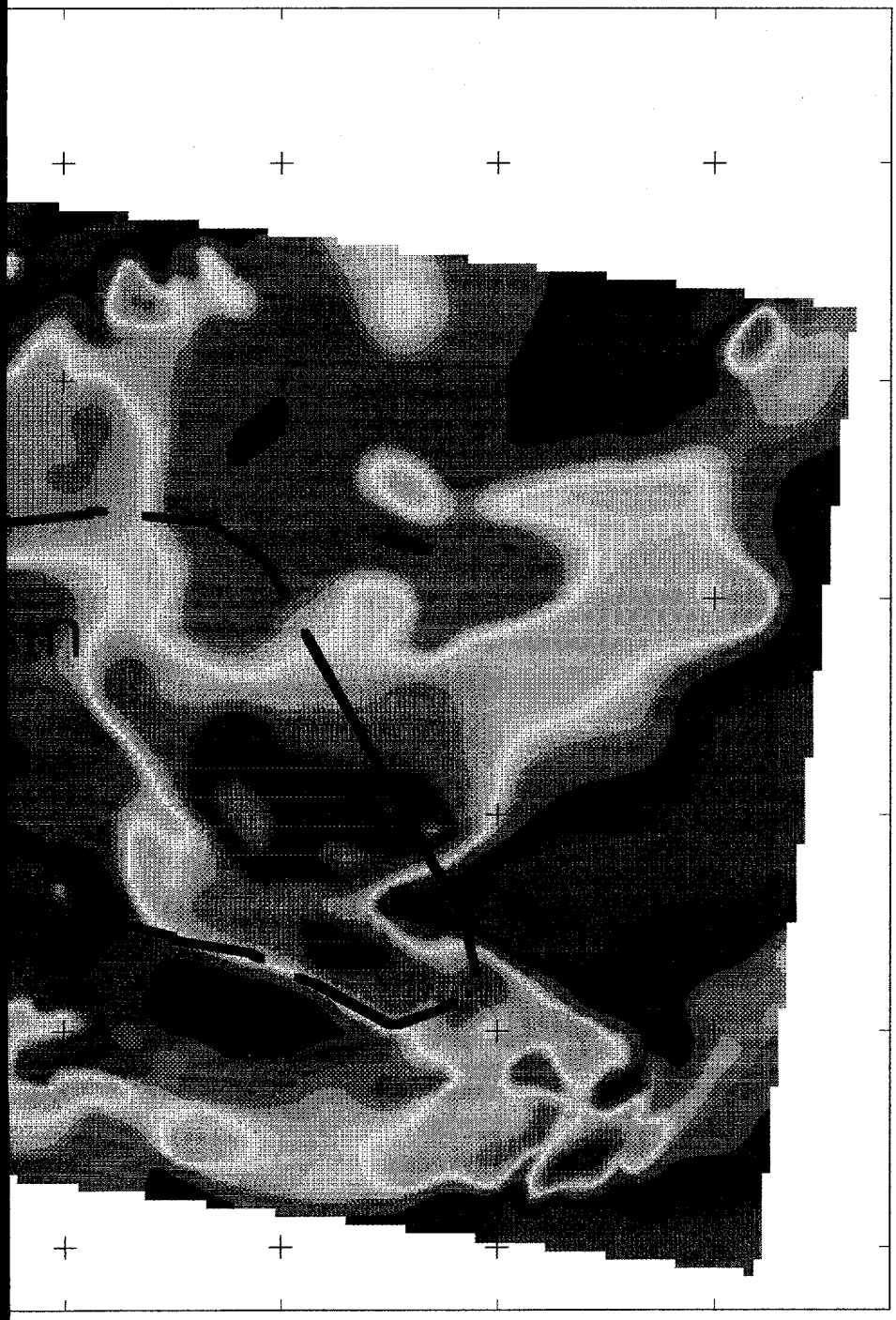

350.
337.
323.
310.
296.
283.
269.
256.
242.
229.
215.
202.
188.
175.
162.
148.
135.
121.
108.
94.
81.
67.
54.
40.
27.
13.
0.
-13.
-27.
-40.
-54.
-67.
-81.
-94.
-108.
-121.
-135.
-148.
-162.
-188.
-202.
-215.
-229.
-242.
-256.
-269.

gammas
regional base removed

N

Scale 1:500000

25000 0 25000 50000 75000 100000

METERS

BLACKHAWK GEOSCIENCES

TOTAL MAGNETIC INTENSITY CONTOUR MAP

WIND RIVER BASIN WYOMING

FIGURE 3-1A

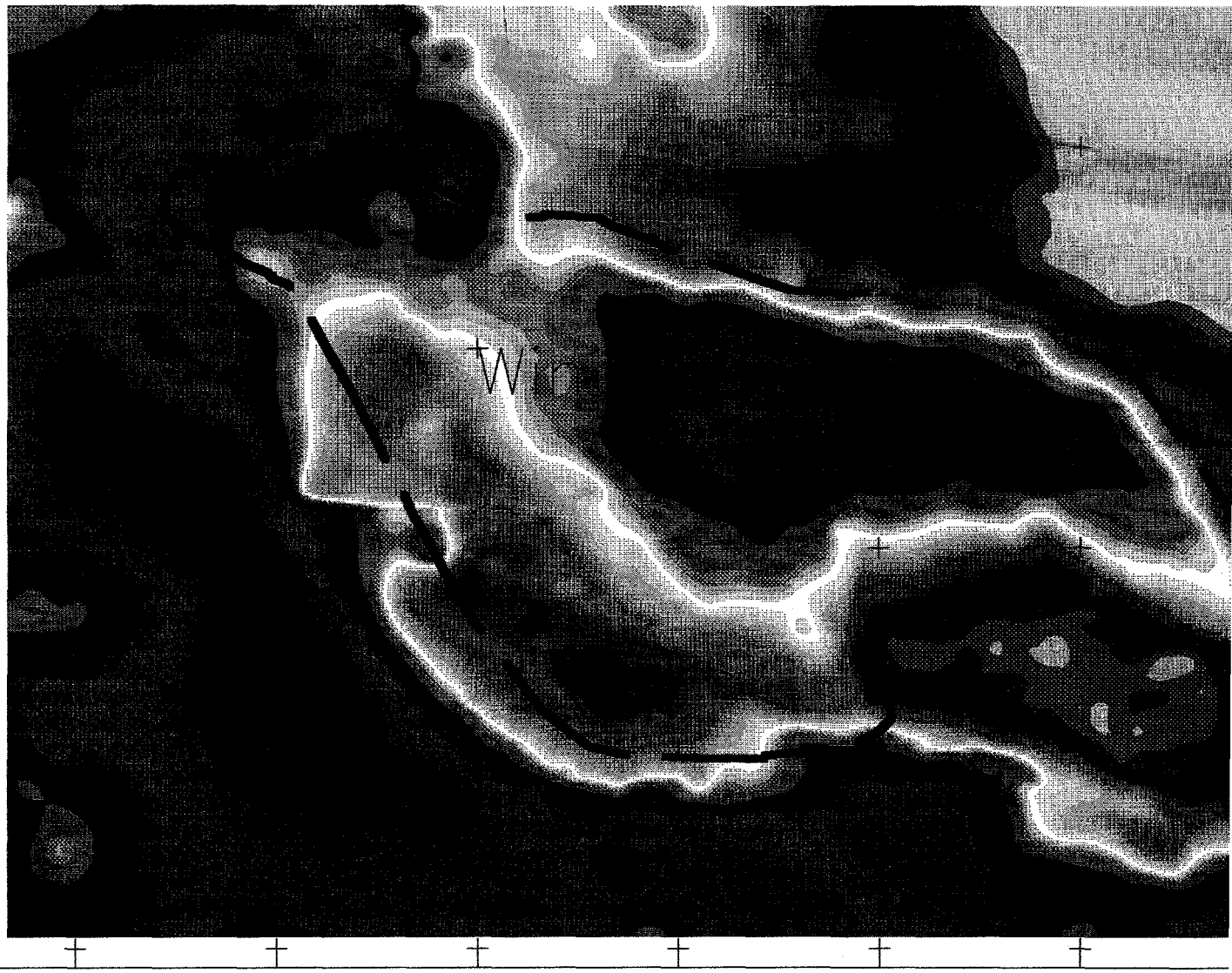

Scale 1:500000

25000 0 25000 50000 75000 100000

Meters

GRAVMASK.GRD
PROJECTS\MAD\QTR4-96\GRAVFNL.PLT

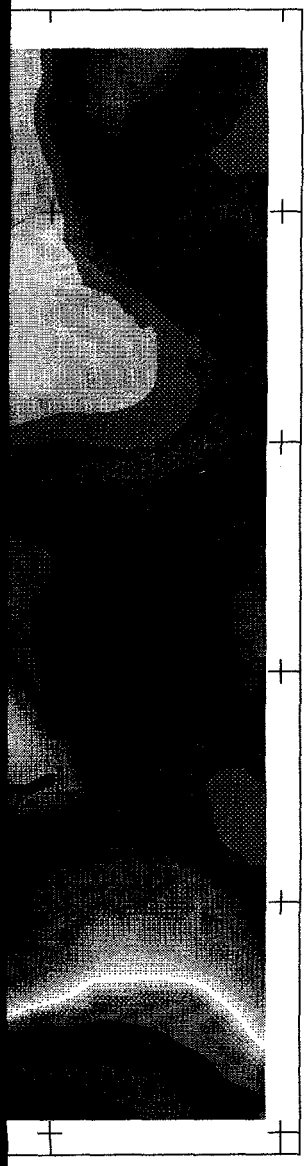

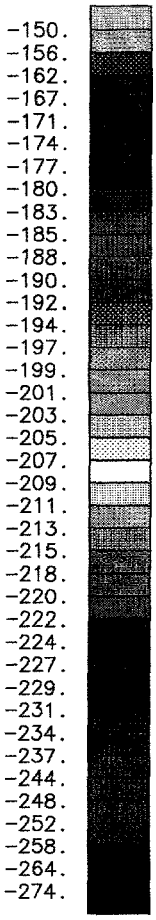

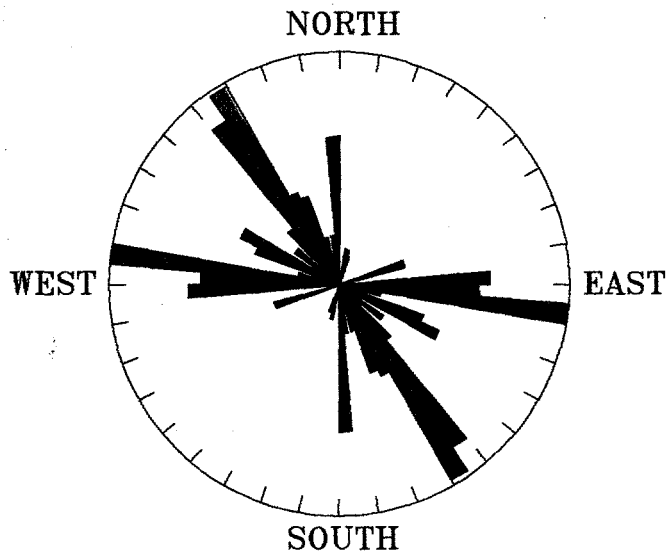

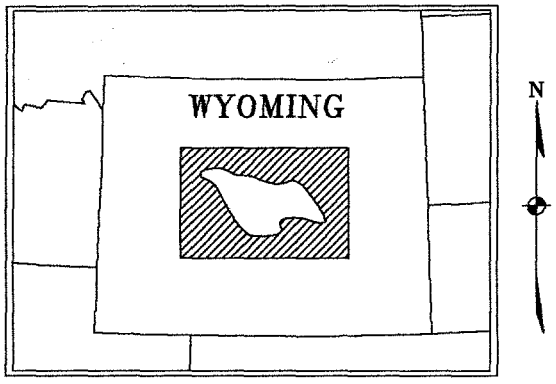

WIND RIVER BASIN
LOCATION MAP

BLACKHAWK GEOSCIENCES

SIMPLE BOUGER GRAVITY AREA MAP
WIND RIVER BASIN WYOMING

FIGURE 3-1B

AIR PHOTOGRAPHY STUDY

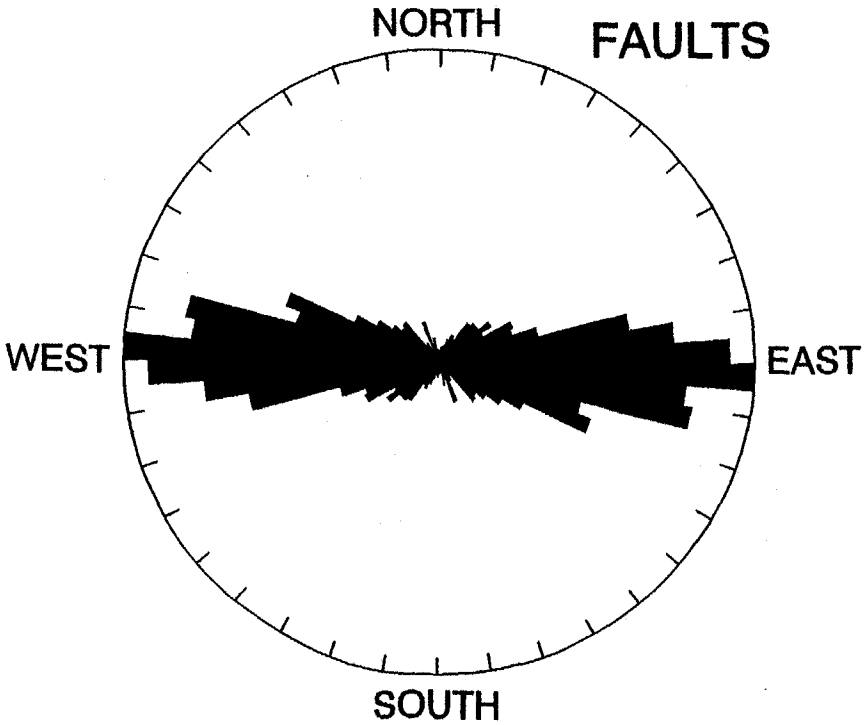

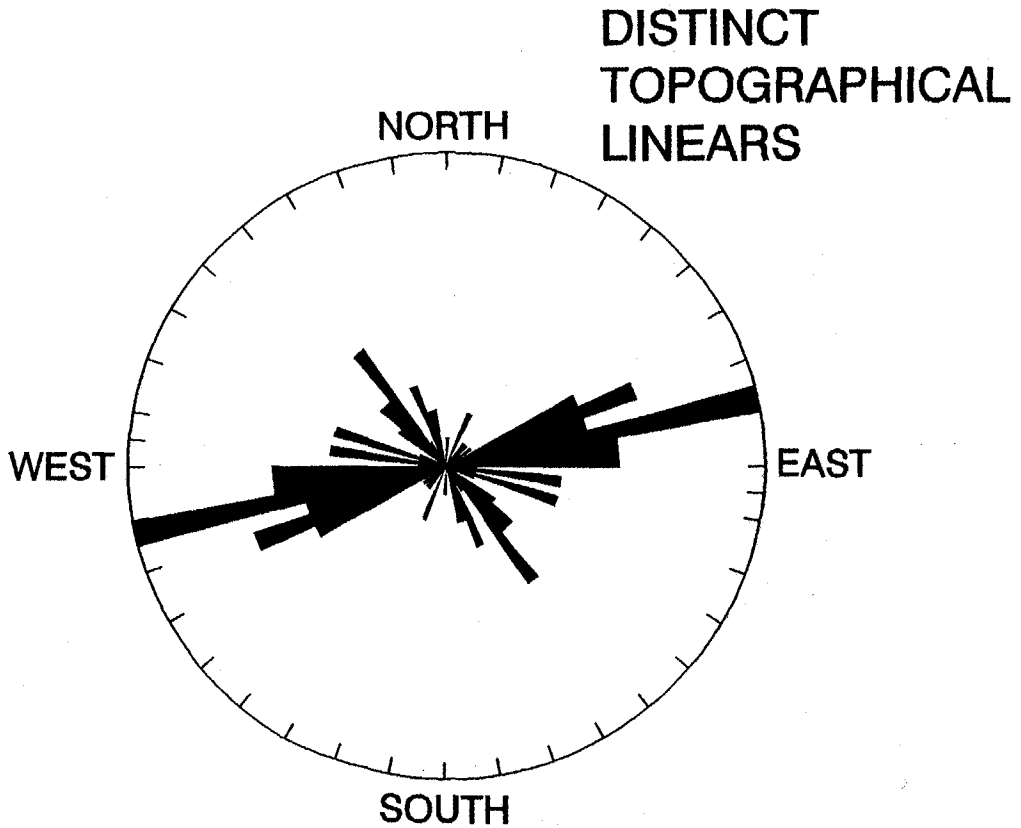

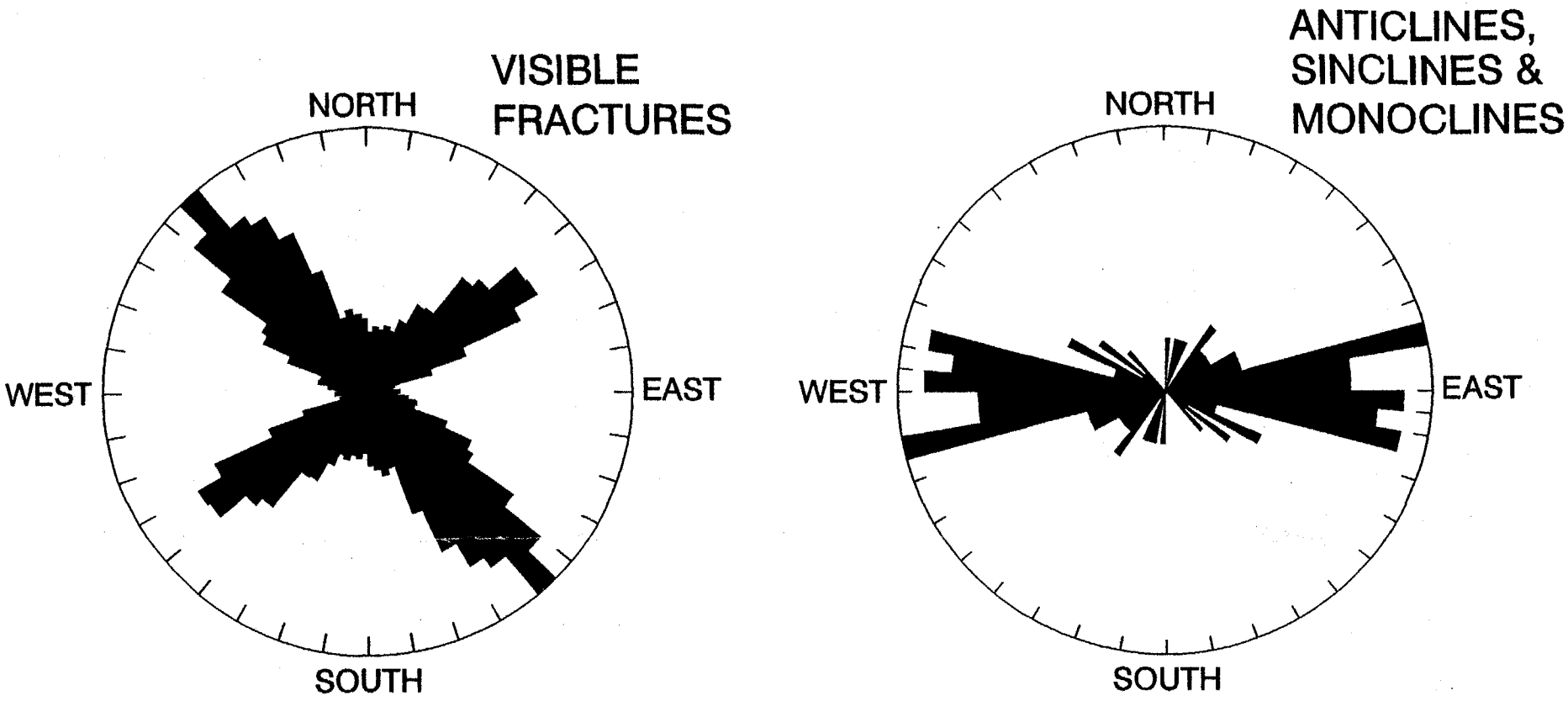
VISIBLE
FRACTURES
NORTH
WEST
EAST
SOUTH
ANTICLINES,
SINCLINES &
MONOCLINES
NORTH
WEST
EAST
SOUTH

FIGURE 3-2

U.S.G.S. REGIONAL STUDY

WYOMING

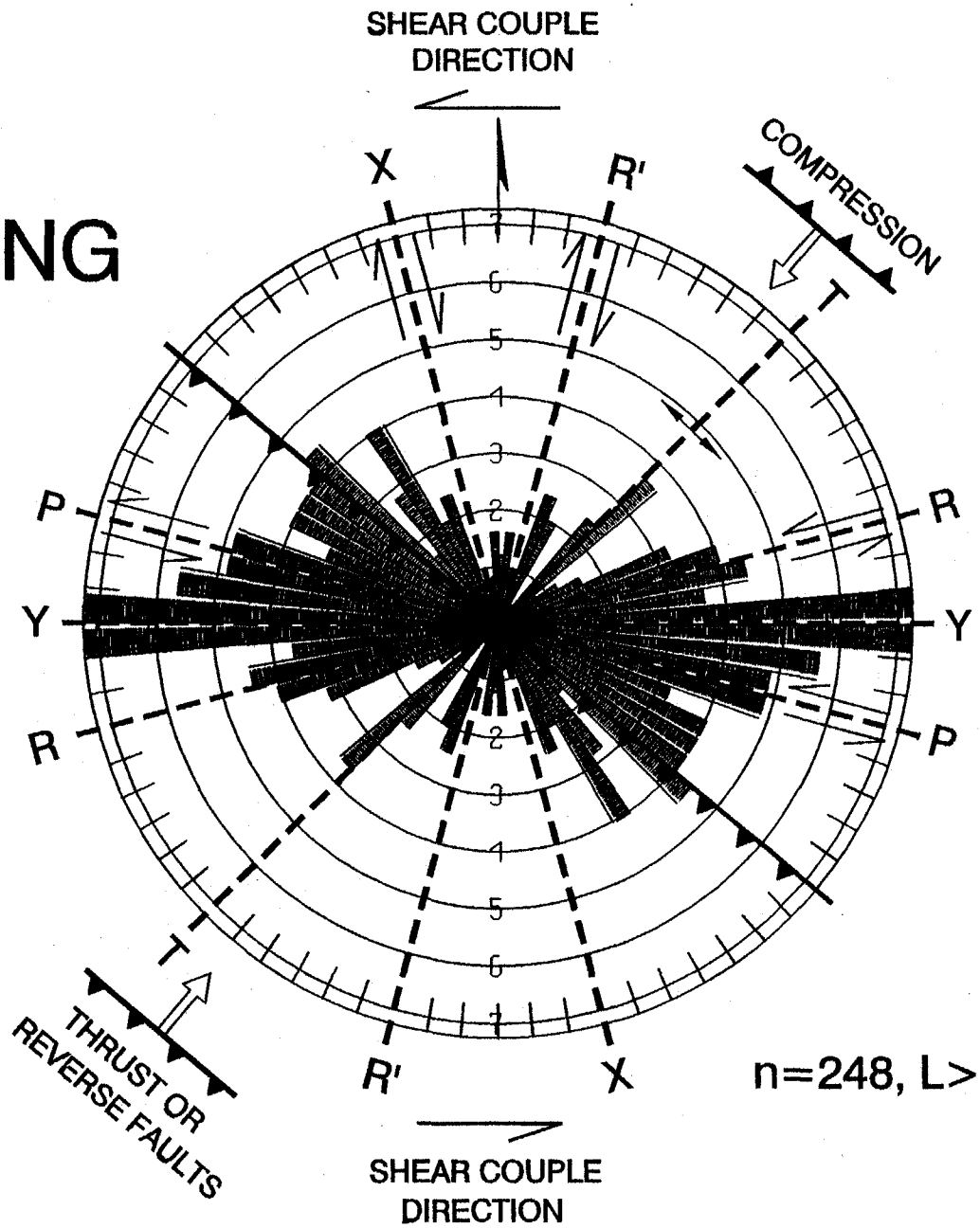

n=248, L>12.5 miles

FIGURE 3-3

SMALL SCA

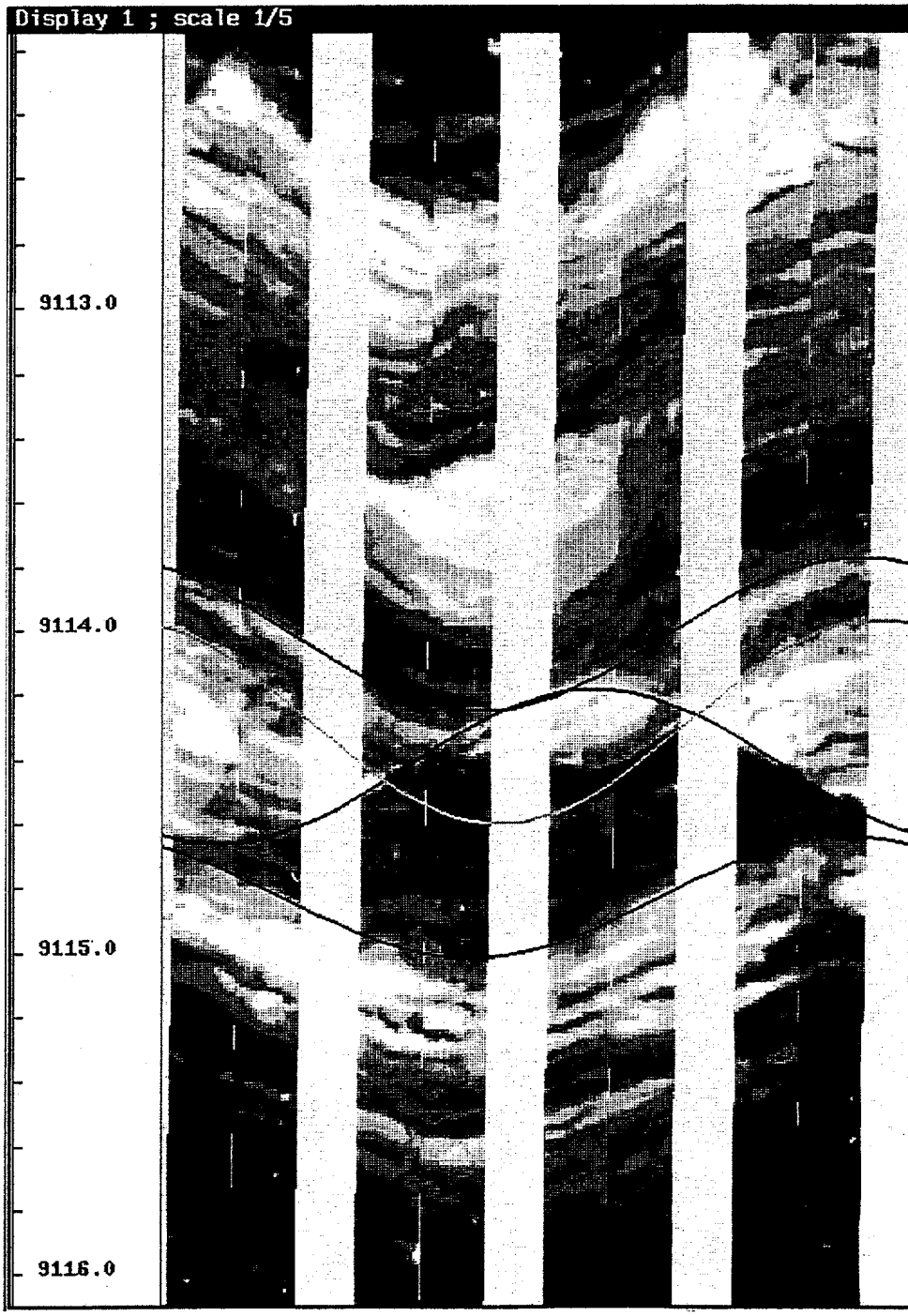

LE FAULTING

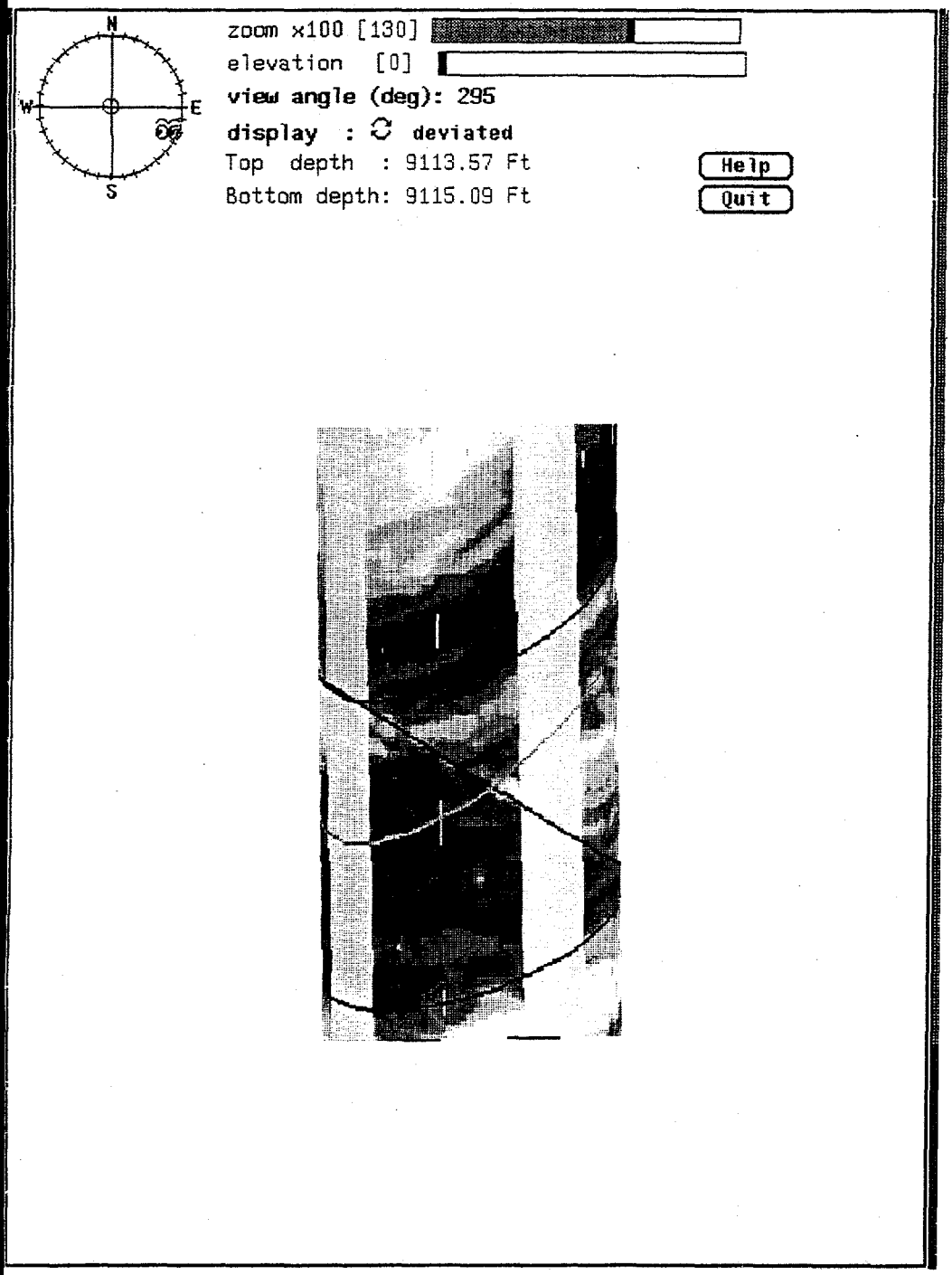

FIGURE 3-4

NEAR VERTIC
EAST-WE

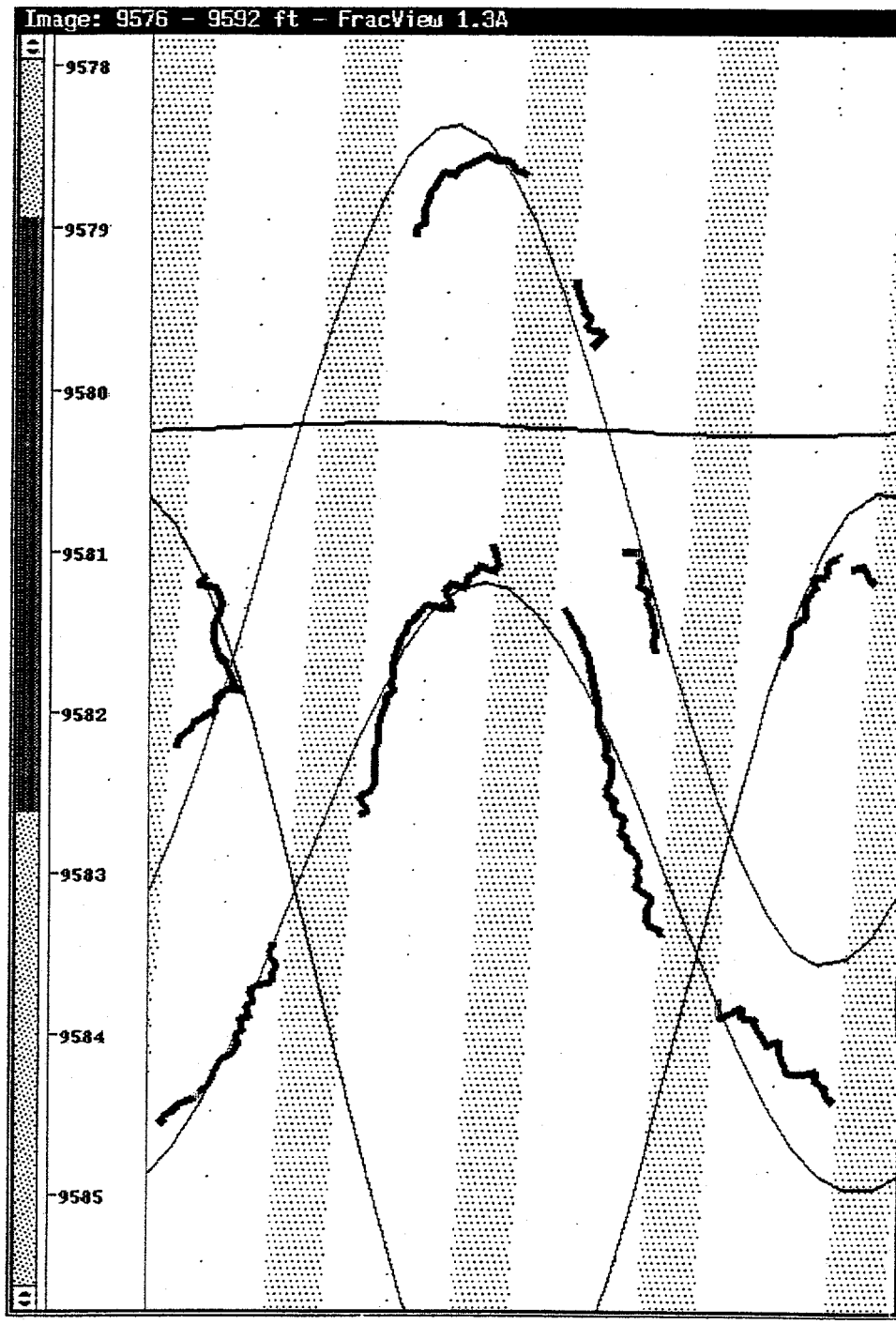

AL FRACTURES
ST STRIKE

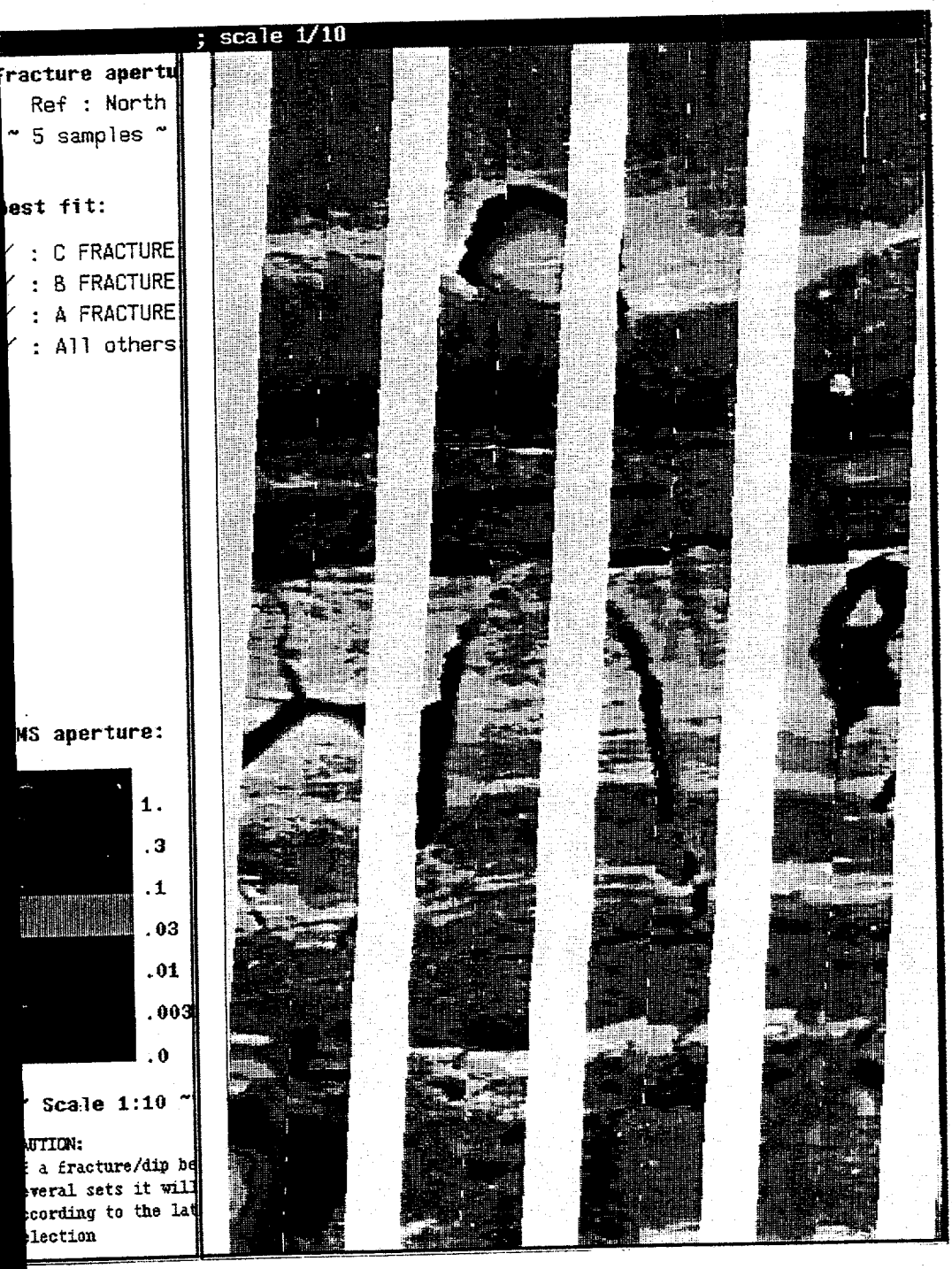

FIGURE 3-5

FRACTURE ANALYSIS FROM FMI LOGS - WELL D-5

5343.0 - 5927.0 ft.
51 SAMPLES

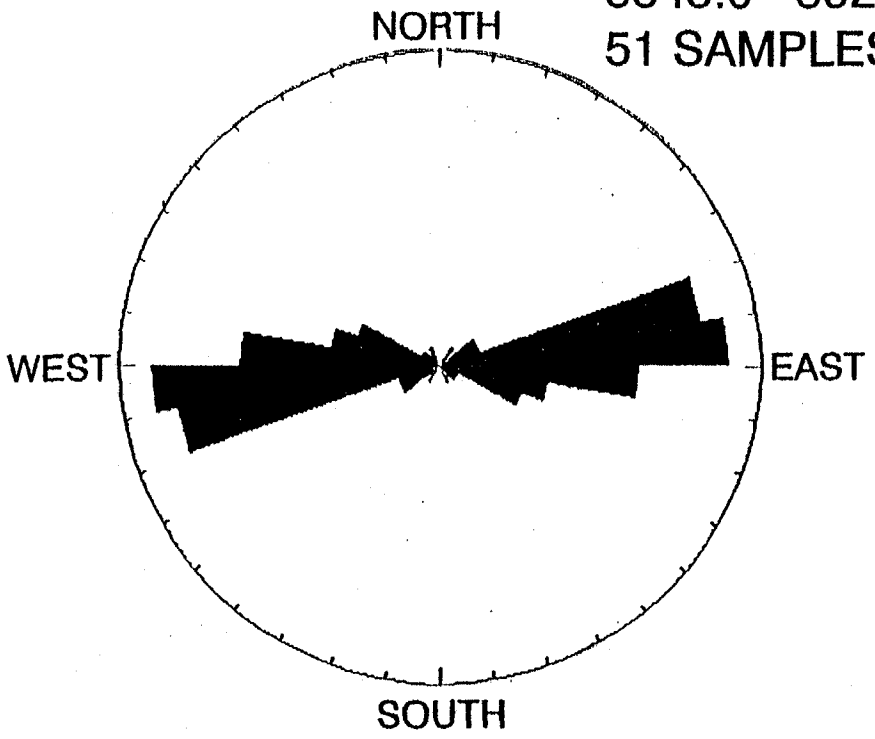

5927.0 - 6943.0 ft.
52 SAMPLES

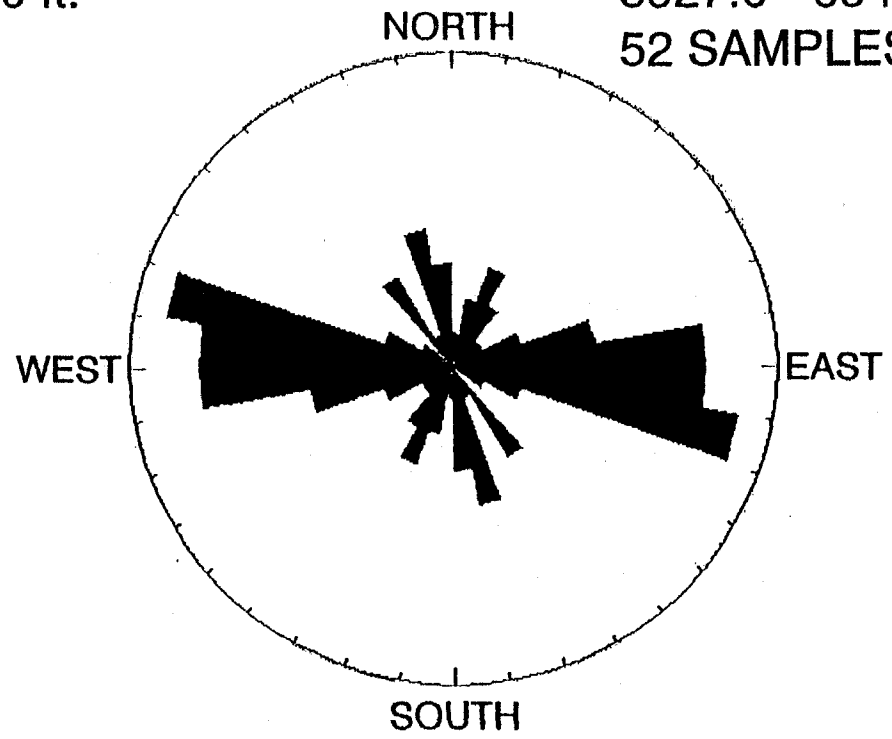

6943.0 - 7853.0 ft.
50 SAMPLES

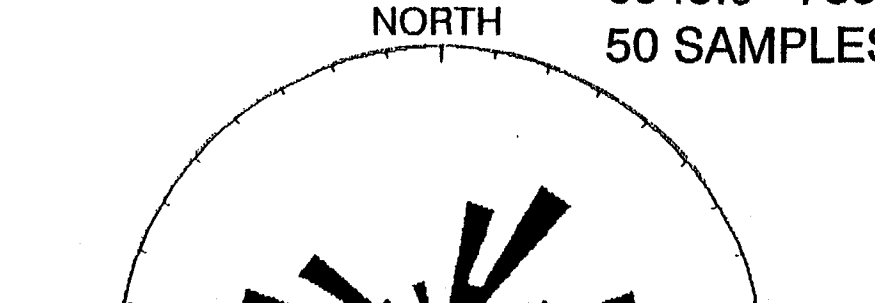

7853.0 - 8509.0 ft.
30 SAMPLES

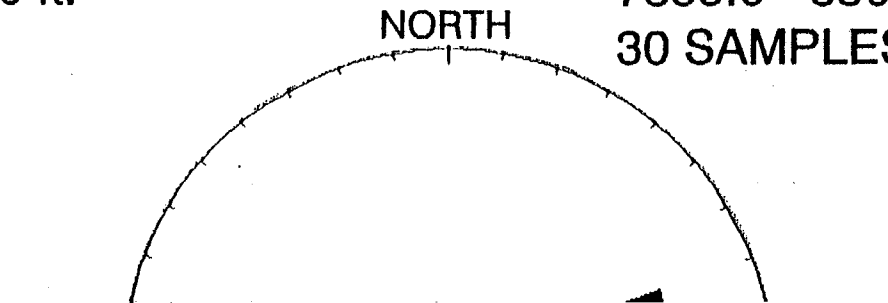

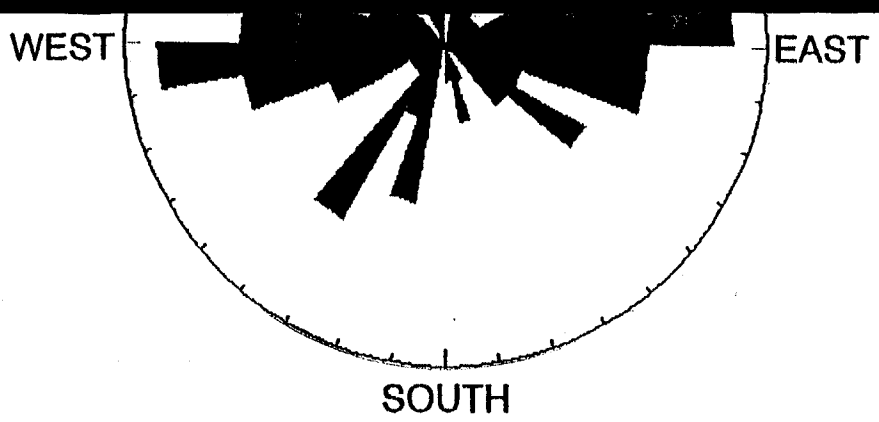

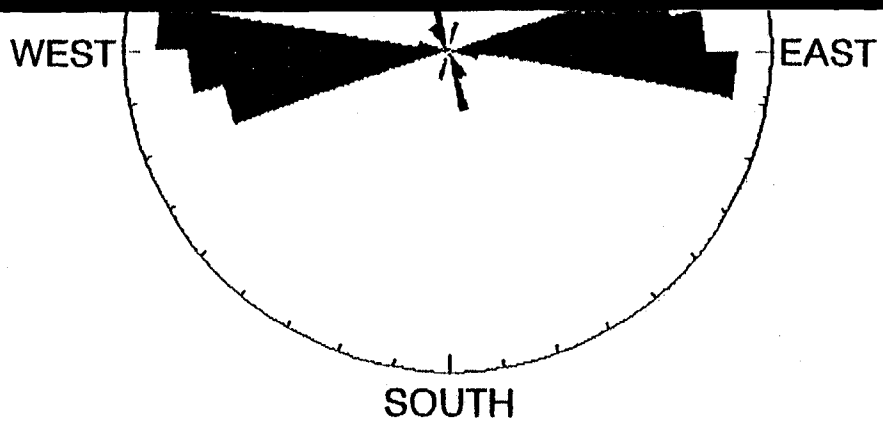

8509.0 - 9200.0 ft.
22 SAMPLES

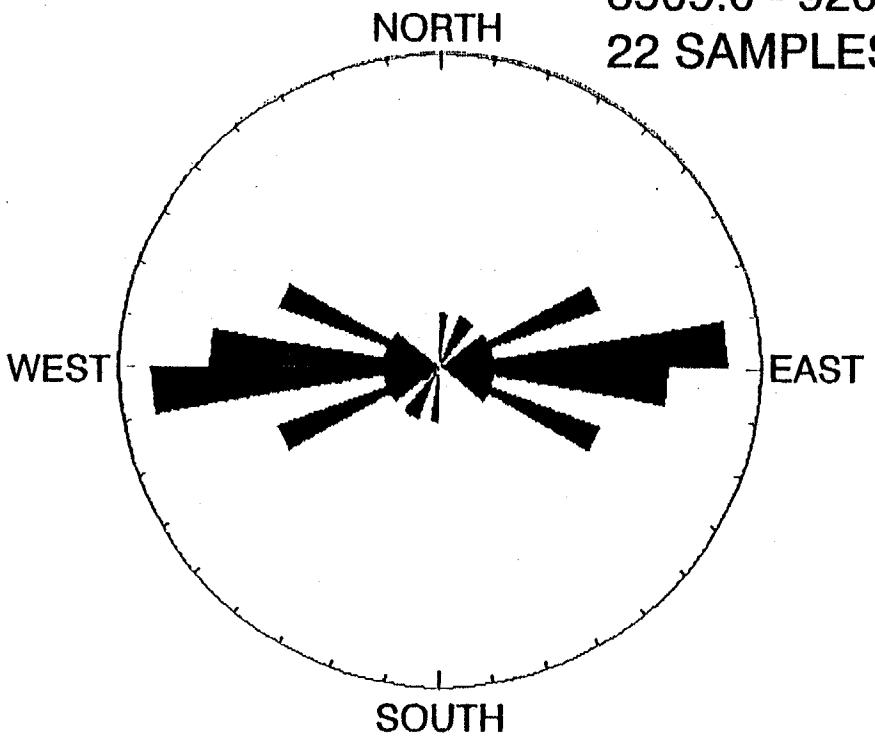

5290.0 - 9650.0 ft.
232 SAMPLES

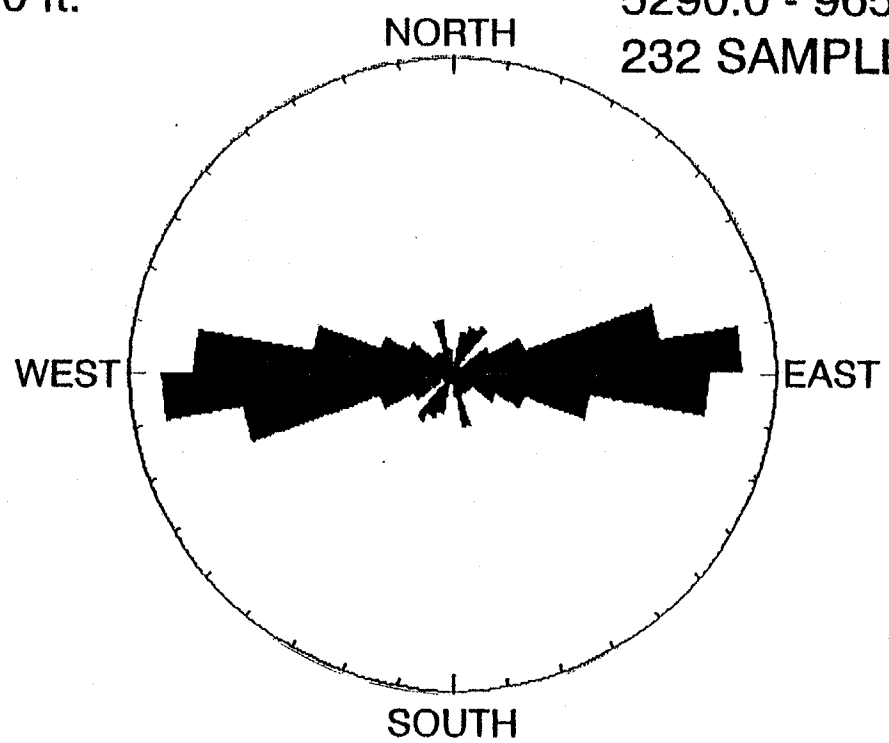

FIGURE 3-6

FRACTURE ANALYSIS FROM FMI LOGS

WELL D-5
5,290 - 9,650 ft.
232 SAMPLES

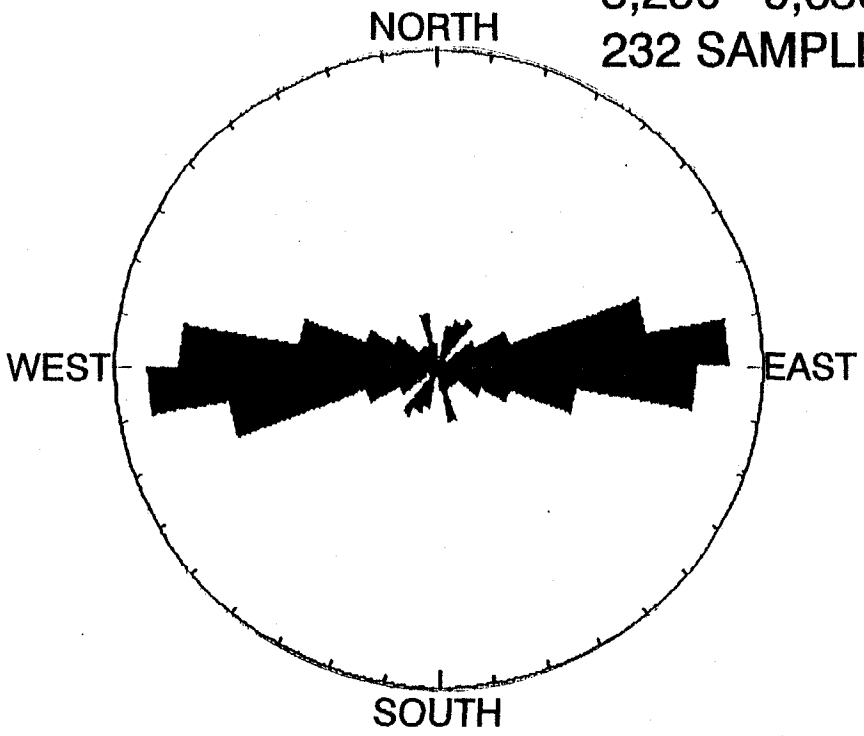

WELL D-19
5,842 - 7,625 ft.
14 SAMPLES

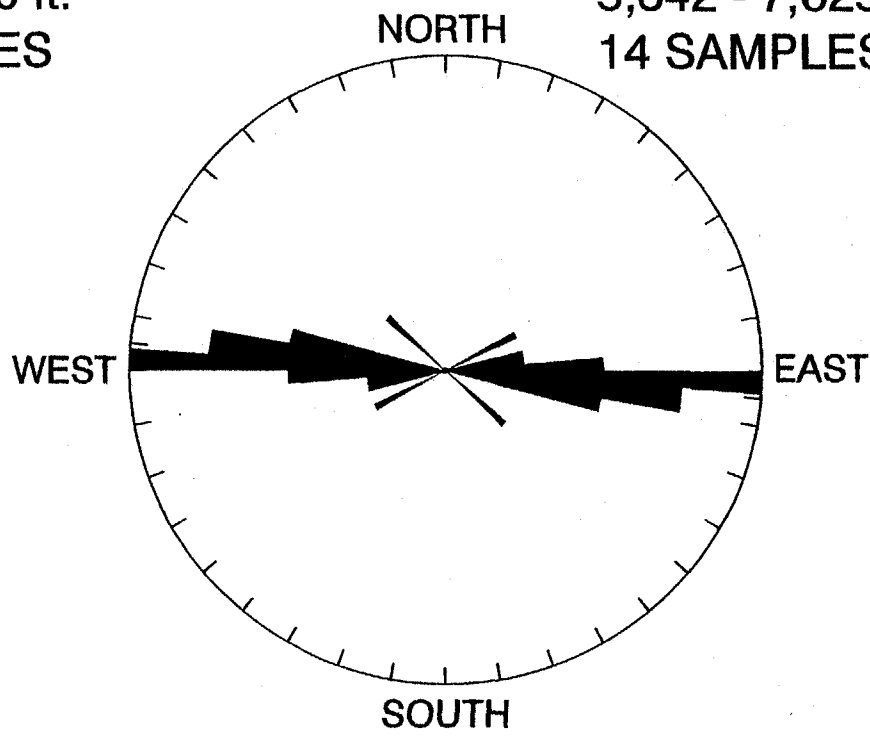

WELL D-10
8,515 - 10,107 ft.
17 SAMPLES

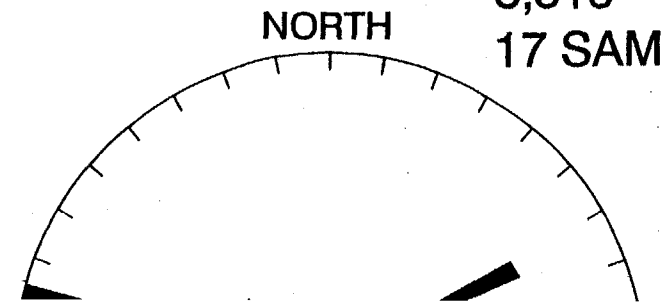

WELL D-8
5,896 - 13,313 ft.
37 SAMPLES

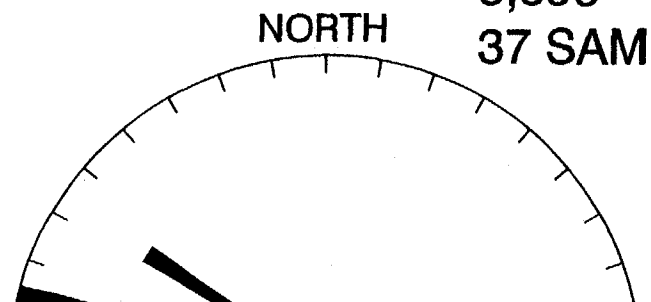

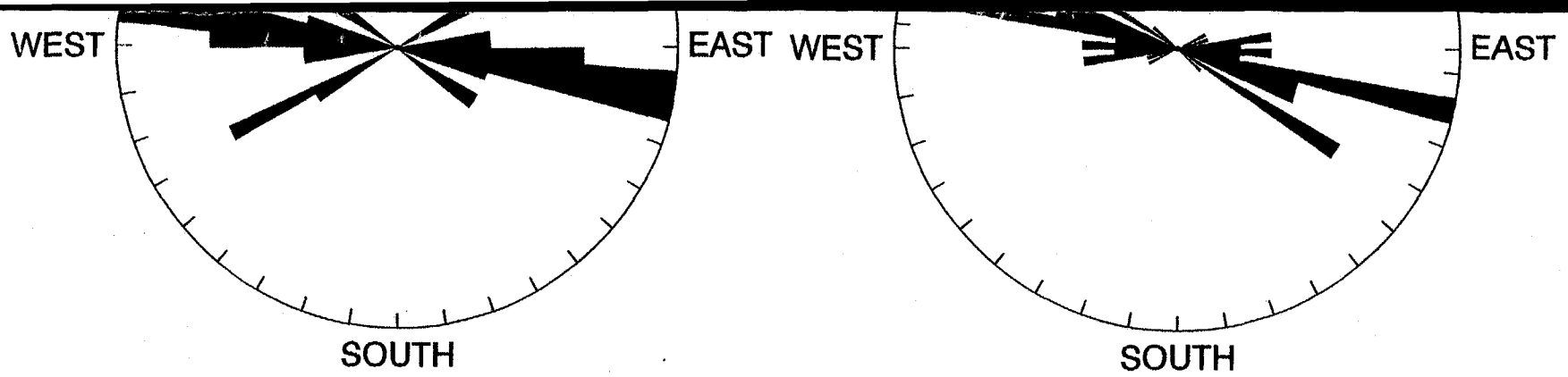

FRACTURE ANALYSIS FROM CBIL LOGS

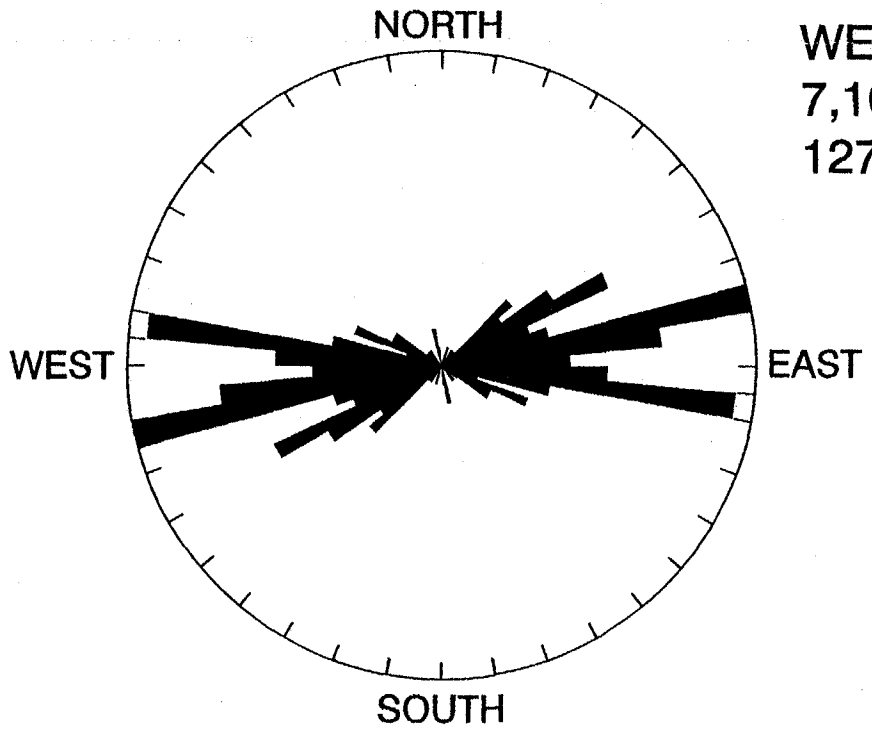

WELL D-17
7,163.59 - 15,793.37 ft.
127 SAMPLES

FIGURE 3-7

FRACTURE ANALYSIS FROM CBIL LOGS - WELL D-17

7163.59 - 8001.56 ft.
33 SAMPLES

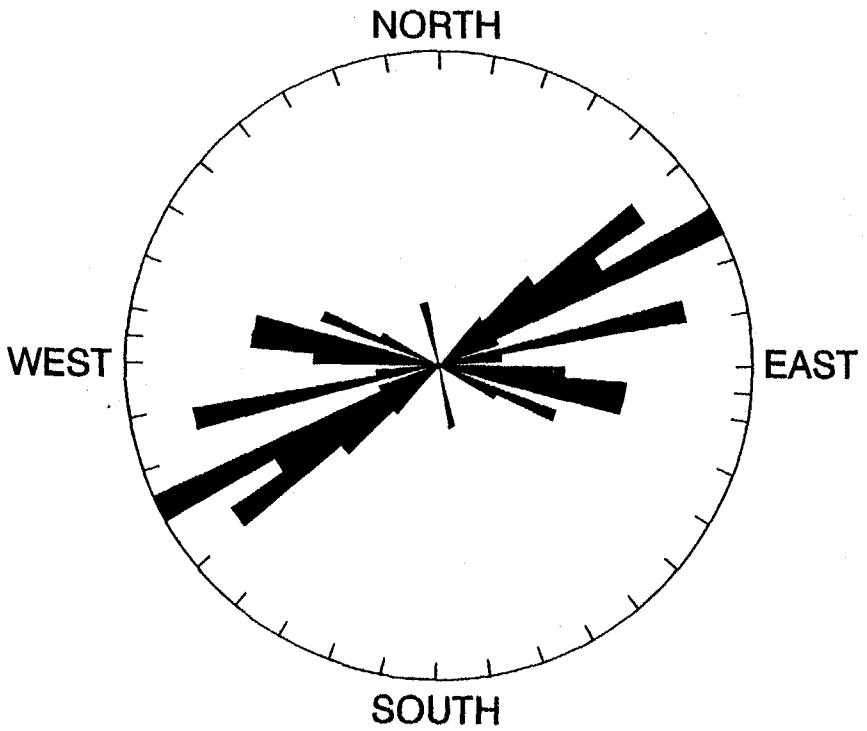

8930.53 - 9788.47 ft.
28 SAMPLES

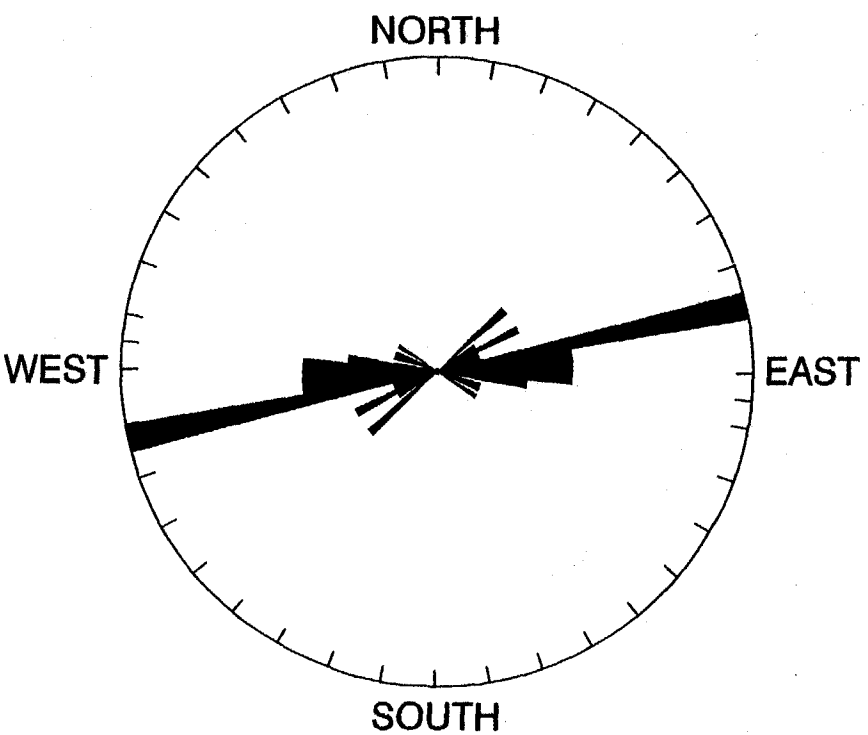

13,078.91 - 15,793.37 ft.
66 SAMPLES

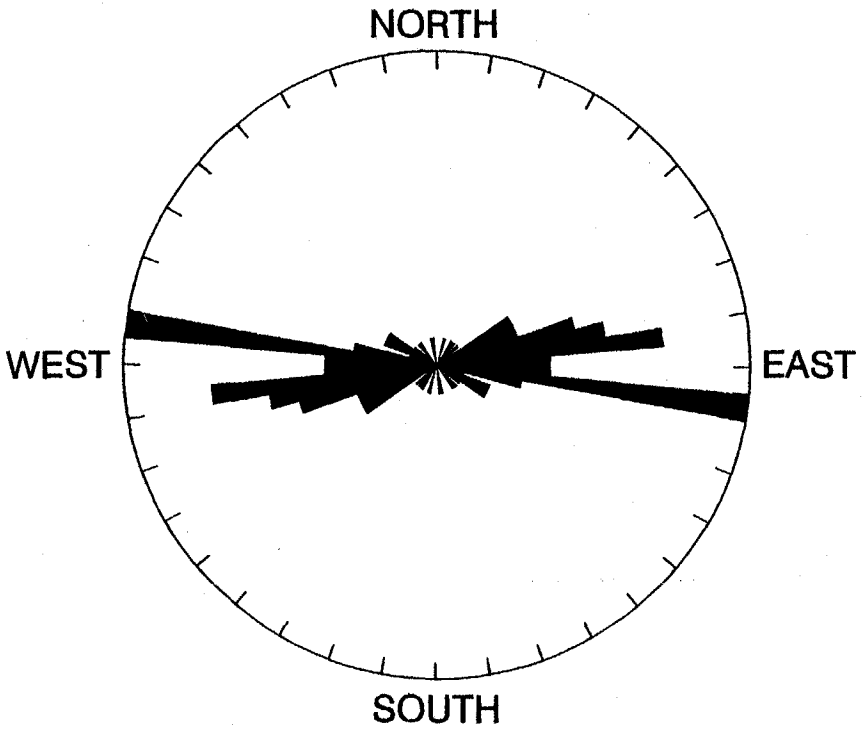

7,163.59 - 15,793.37 ft.
127 SAMPLES

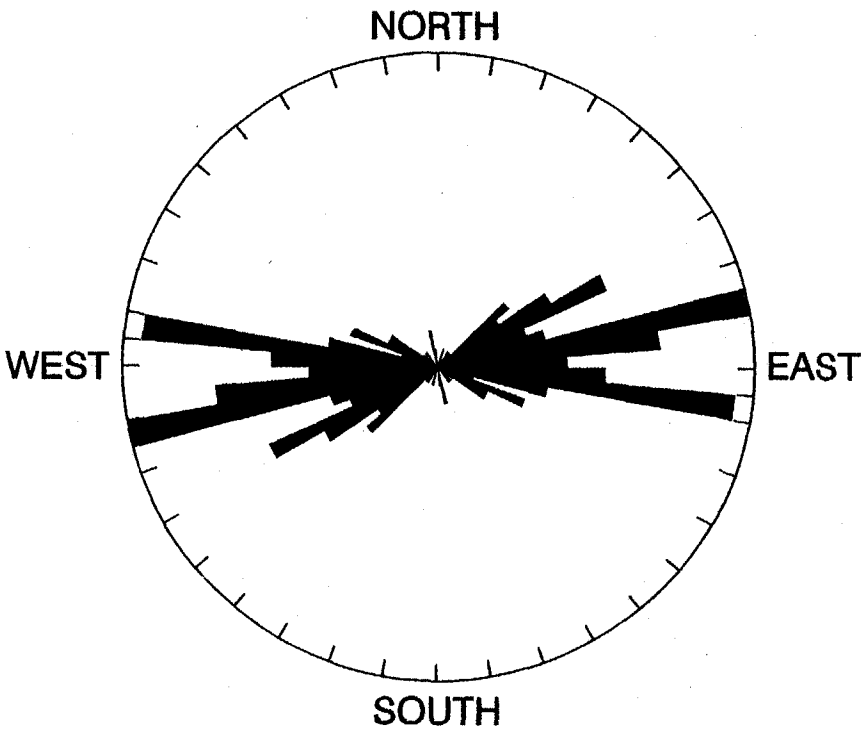

FIGURE 3-8

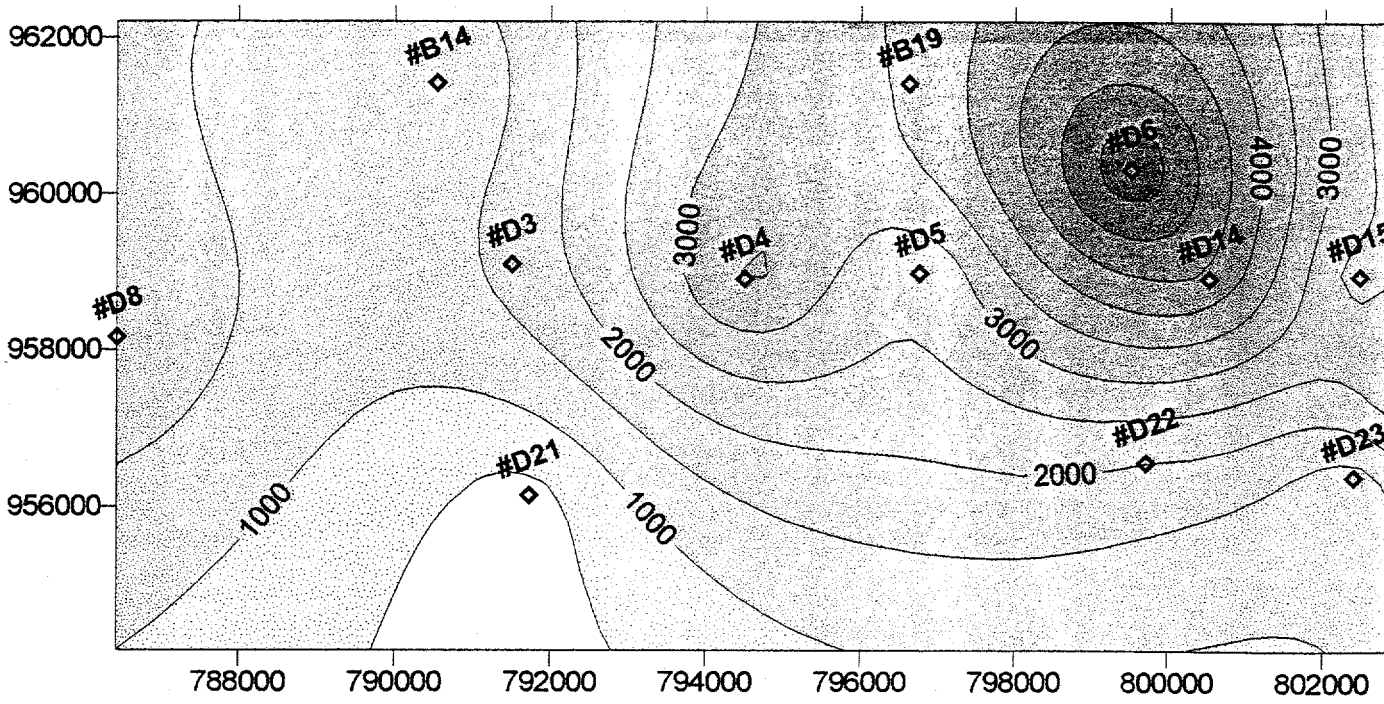

a) First 6 months produ

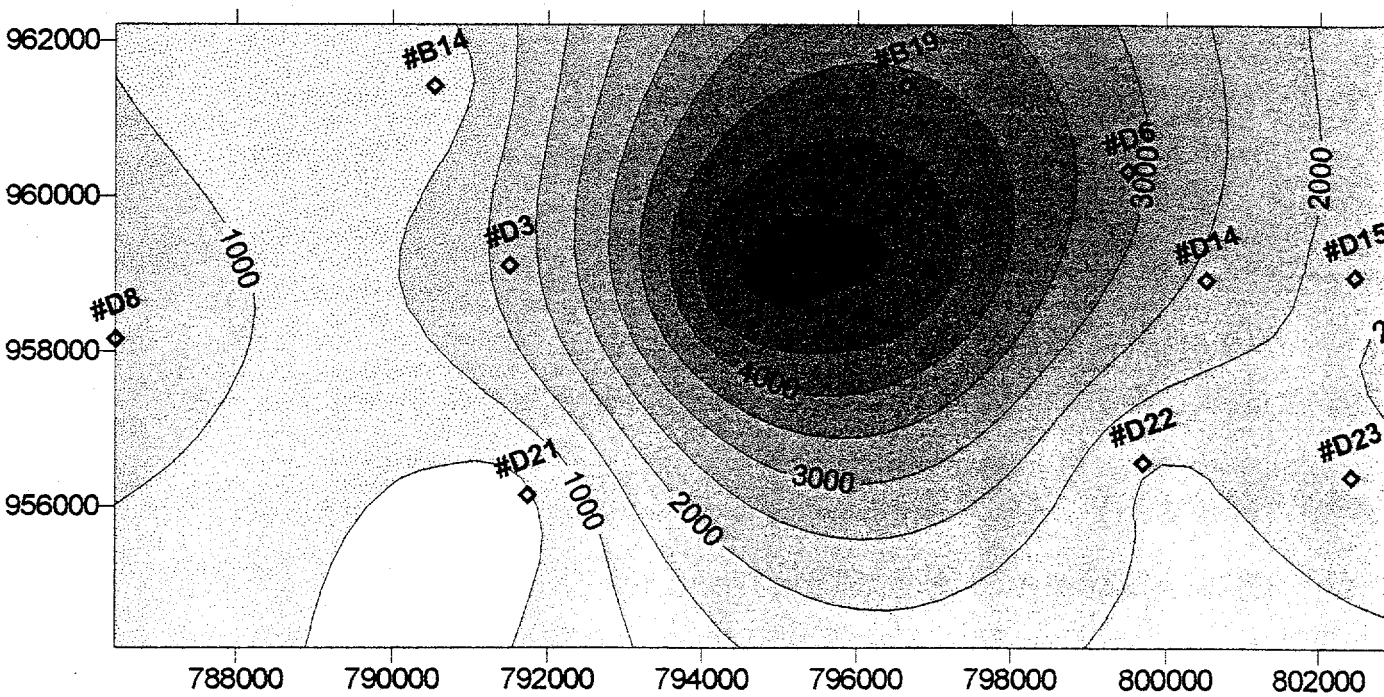

b) Production from L

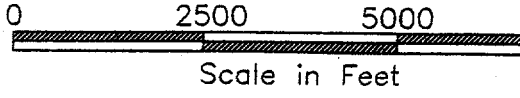

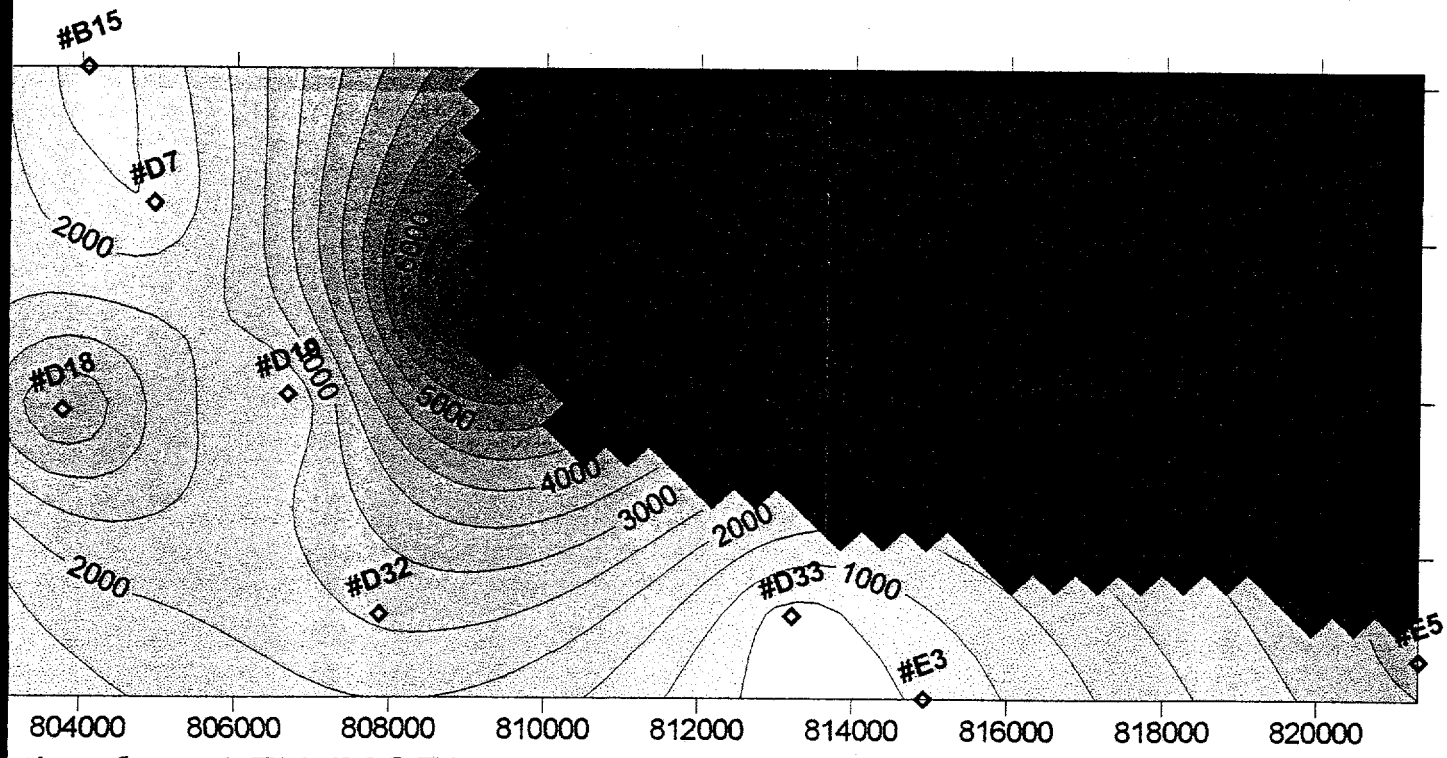

ction from LFU (MCF/day)

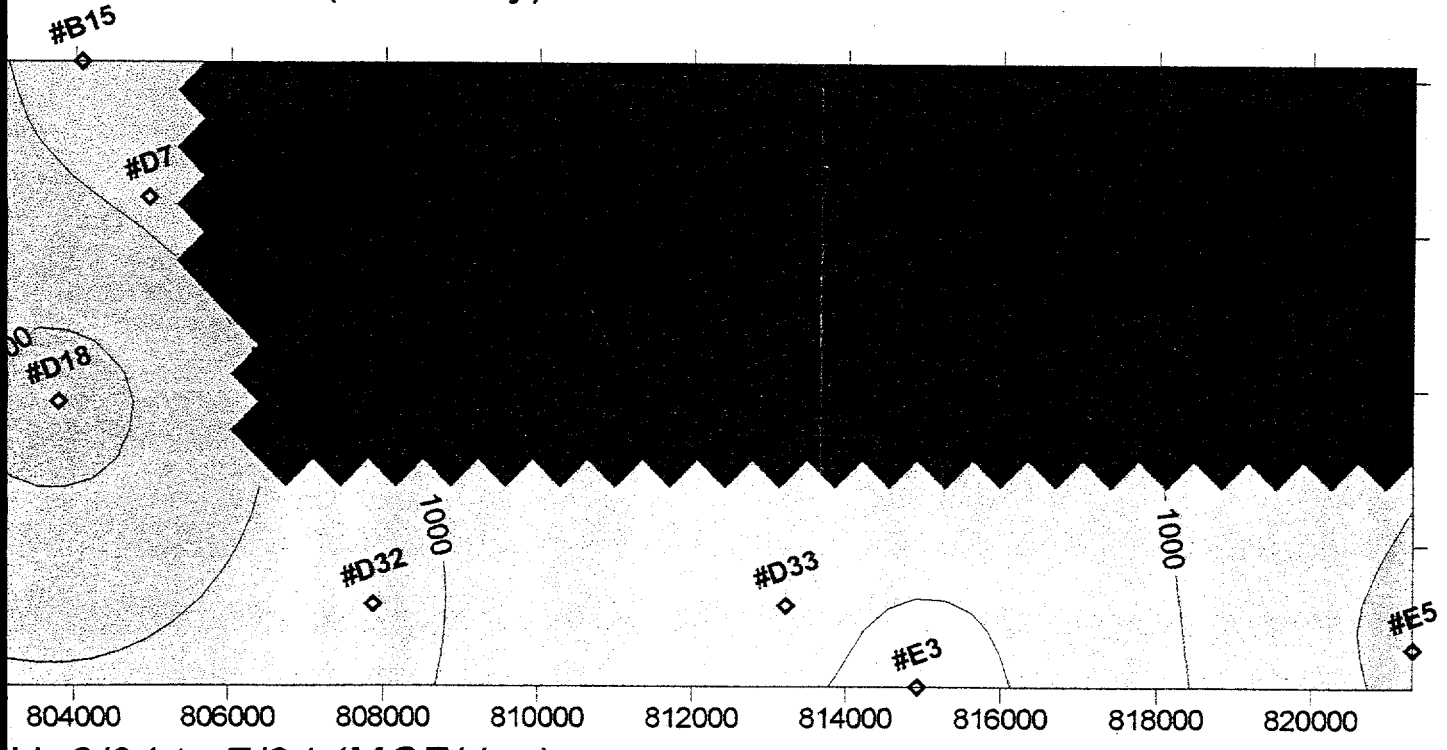

U 2/94 to 7/94 (MCF/day)

7500

N

BLACKHAWK GEOSCIENCES

GAS PRODUCTION
FROM
LOWER FORT UNION

FIGURE 3-9 A&B

1993-94 REPEAT

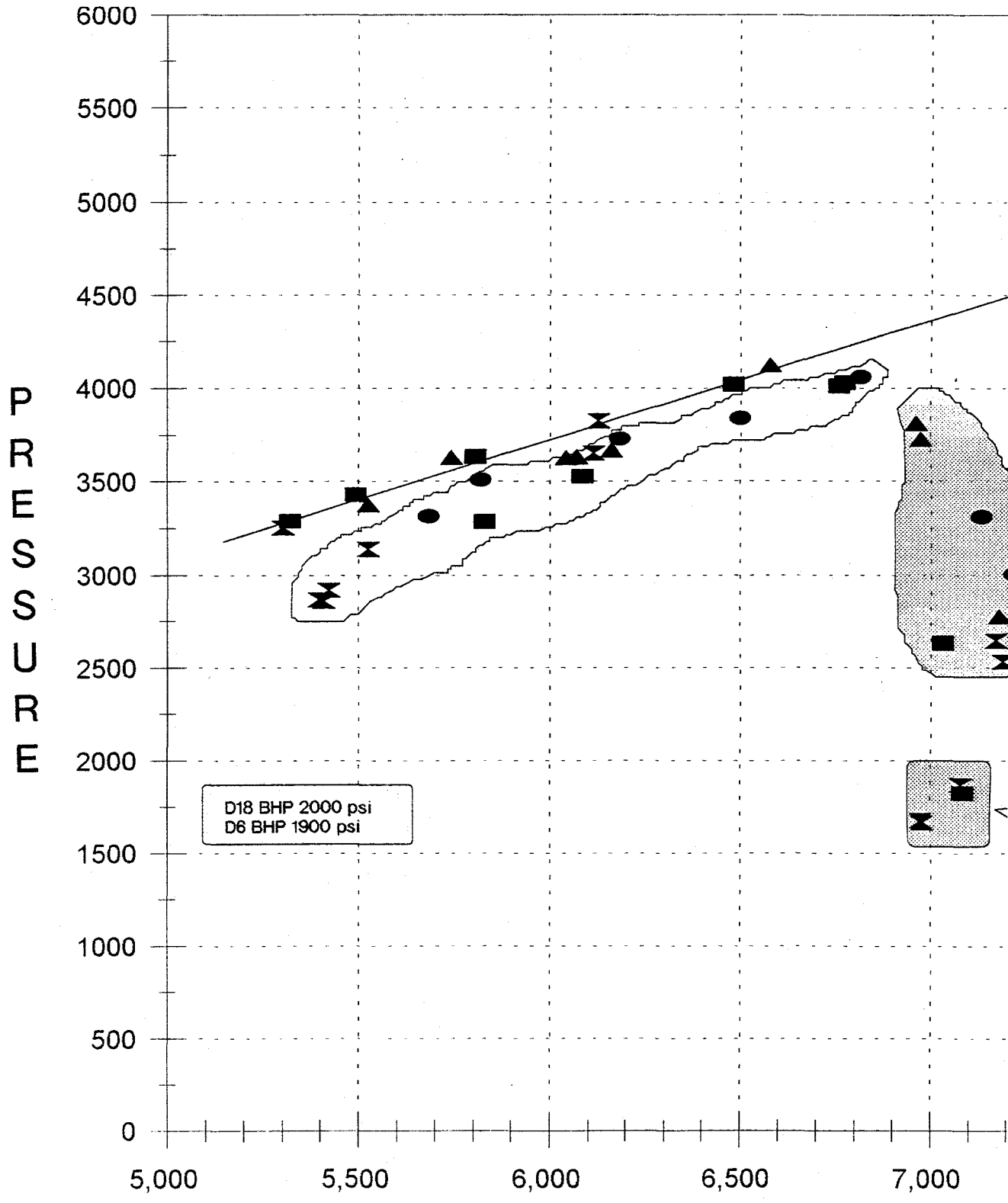

FORMATION TEST DATA

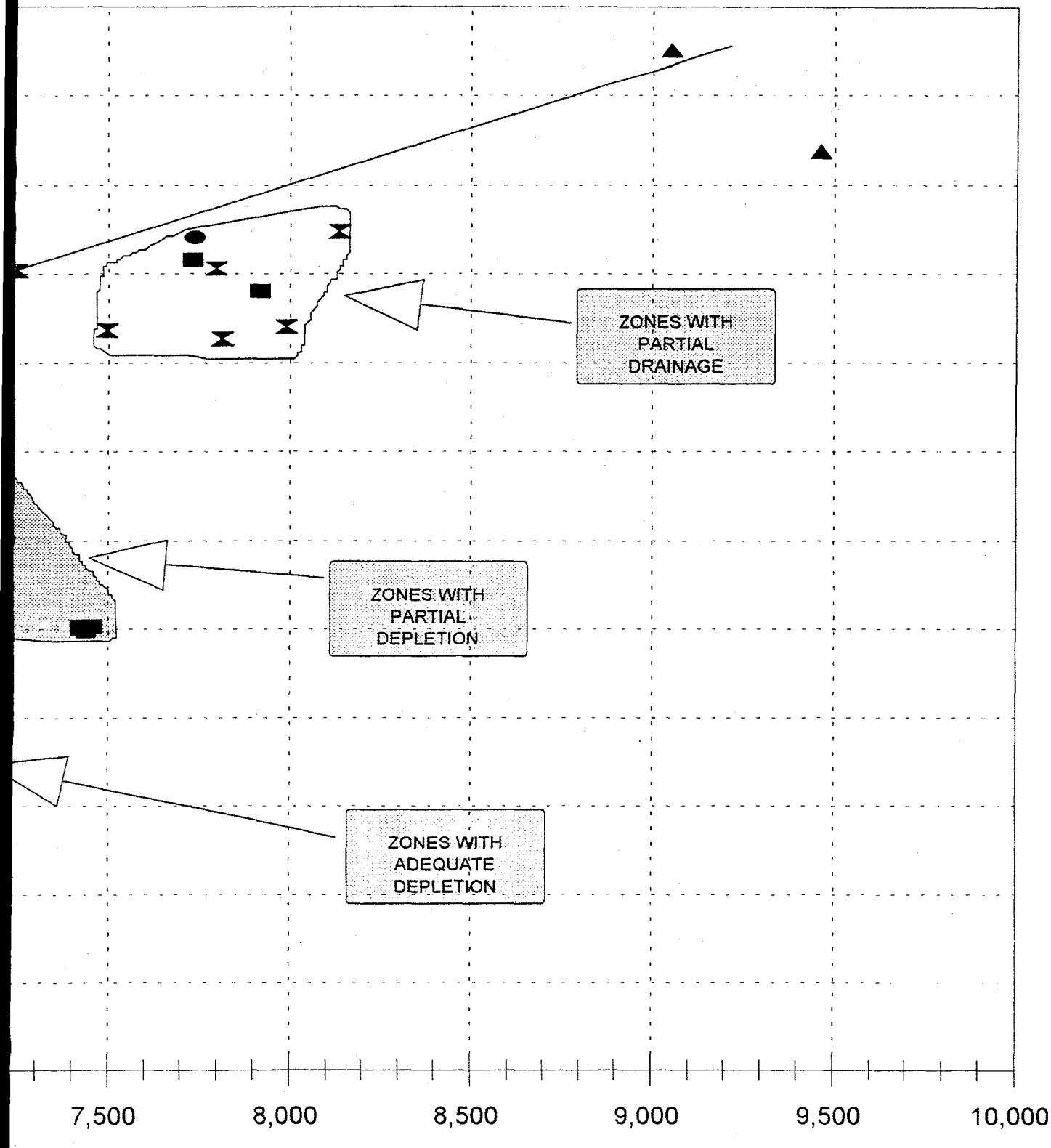

FIGURE 3-10

4.0 3D-3C Seismic Processing

A request for bid for the 3D-3C seismic data was made in January. The principal goals of the 3D-3C are:

- Structural Mapping of reflectors between 0.8 sec and 2.8 sec (lower Fort Union).
- Map view of fast shear wave (S1) orientation to predict open fracture azimuth.
- Map view of relative fracture density in the reservoir (mapping the magnitude of seismic anisotropy).

Ten companies were identified as potential responders to the bid requests. Of these, it was felt that only two companies showed the required knowledge to adequately address the complex processing. Western geophysical was selected for a number of reasons.

Western Geophysical, located in Denver, processed the original 3D P-wave data and are not only familiar with the data area, but are also familiar with the technical requirements for both tasks outlined in the 3D P-wave processing. It is our opinion that Western is the most technically qualified processing company for these tasks. Furthermore, Western is familiar with the owner/operators concerns with the proprietary nature of the data. Western has provided highly competitive pricing. Also, as they are a U.S. company, their grading puts them first for the P-wave tasks.

For processing the mode converted data, Western has a highly qualified technical staff with experience in 2D and 3D processing, but they have not to date completed any 3D mode converted projects using the processing steps outlined in the request for bid. Specific to these are the common conversion point binning (CCP) and mode converted/shear wave DMO. Western has recently joined the CREWS consortium that has written the original software for these types of processes. Thus, Western will have the necessary code running and tested before the actual data must be processed. It is our opinion that despite their lack of experience in these specific aspects, Western will be capable of producing the end results required of them. Furthermore, Western has indicated it is making a dedicated effort to develop its experience in this type of data processing as it foresees a market for the services in the future. Western will be the only US company providing the service in the future.

Negotiation began with Western in mid-March. Western received all the data tapes at the end of March and verified that they were able to read the data. Processing shall begin in early April after a kick off meeting to review the processing details. Western will be required to follow a strict time schedule for the processing in order to allow sufficient time at the end of the project for interpretation and integration of the data. The time schedule for both P-wave and mode converted processing is given below in Tables 4.1 and 4.2.

TABLE 4.1 P-P PROCESSING Receipt of Tapes and All Support Data (Survey Elevations, OB Notes).	
Start Date	Verification of readability of tapes.
By End of 1st Week	First estimate of amplitude adjustments, deconvolution.
By End of 3rd Week	Initial stacks; review gathers, second pass statics, velocity. P-wave source statics provided to P-S processing contractor.
By End of 4th Week	Final stacks. Initial migrations. Final migrations. Review
By End of 5th Week	Azimuth bin gathers, 25 per square mile (about every 1000 ft). Pick velocities as function of azimuth and time. Review bin gathers. Interpolate velocities to build volume.
By End of 6th Week	Apply velocities, and pick maximum/minimum amplitude azimuths and maximum/minimum velocity azimuths as function of (x,y,t) for key reflectors (T/Waltman, T/LFU, 2 within LFU, T/Lance, 2.5 sec (mid-Cretaceous) reflector.
By End of 7th Week	Calculate AVO gradient in principal azimuths for every CDP bin. Calculate difference in AVO gradients for entire volume.

Table 4.2 P-S PROCESSING Receipt of Tapes and All Support Data (Survey Elevations, OB Notes).	
Start Date	Verification of readability of tapes.
By End of 2nd Week	First estimate of amplitude adjustments, S1/S2 azimuths; deconvolution.
By End of 4th Week	Separate volumes into N6SE and N155E (±30), also, N95E and N27E5E (+/- 30°), apply DMO, pick DMO velocities on Common Conversion Point data; estimate statics; stack.
By End of 6th Week	Review gathers, second pass statics, velocity.
By End of 8th Week	Final stacks. Initial migrations. Review migrations.
By End of 9th Week	Final migrations. Review migrations.
By End of 10th Week	Azimuth bin gathers, 25 per square mile (about every 1000 ft). Pick velocities as function of azimuth and time. Review gathers. Interpolate velocities to build volume.
By End of 12 Week	Apply velocities, and pick maximum/minimum amplitude azimuths and maximum/minimum velocity azimuths as function of (x,y,t) for key reflectors (T/Waltman, T/LFU, 2 within LFU, T/Lance, 2.5 sec (mid-Cretaceous) reflector. Calculate AVO gradient in principal azimuths for every CDP bin. Post difference in AVO gradients

5.0 Technology Transfer

A summary of 1996 technology transfer events is given in Table 5. Also, in appendix A are copies of all papers and abstracts submitted during the first quarter of 1996.

TABLE 5.1

1996 DOE AND RELATED VENTURES TECHNOLOGY TRANSFER PROGRAM

APRIL	• SAGEEP, Keystone, CO. Presentation: "Multi-Component Seismic Acquisition in engineering and Environmental Investigations." • AAPG Annual Convention, San Diego, CA. Presentations: "Open Fracture Prediction and Detection at the Bluebell-Altamont Field, Uinta Basin, Utah," and "Seismic Shear Wave Investigations for Fracture Mapping in Bedrock Controlled Hydrology." • Papers Submitted to the Leading Edge Special Edition on "Correlation Between P-Wave AVO Anisotropy, S-Wave Travel Time Anisotropy in a Naturally Fractured Gas Reservoir," "Azimuthal Anisotropy in P-Wave 3D (Multi-Azimuth) Data" and "Problems in the Analysis of Multi-Component VSP Data."
JUNE	• Wyoming Geologic Association, Casper, WY, Lower Fort Union Workshop. Presentation on Wind River Basin by Blackhawk Geosciences, "Fracture Indicators for the Lower Fort Union, Wind River Basin, WY," and "3D Multi-Azimuth P-P Reflection Data: Analysis of Azimuth Dependent Seismic Signatures and Their Relations to Production" by Lynn, Inc. • Joint SWPLA, GSH, HGS Workshop on Fractured Reservoirs. Presentation and Poster Paper on "Seismic Characterization of Naturally Fractured Gas Reservoirs" and "Department of Energy Reservoir Characterization Program of Naturally Fractured Gas Reservoirs."
JULY	• AAPG Rocky Mountain Section Annual Meeting.
AUGUST	• Special Issue of "The Leading Edge" on the October, 1995 DOE Technology Transfer Workshop, Houston, TX (Described in April Above).
OCTOBER	• Society of Exploration Geophysicists Annual Convention, Denver, CO. Presentations "Naturally Fractured Gas Reservoirs Seismic Characterization" and "Near Surface Variability in Shear Wave Velocity Anisotropy."

In-House Presentations Are Also Scheduled To Be Made To:

Amoco	ARI	Arco
Mitchell Energy	Barrett	CSM
Anadarko	Snyder	Western Geophysical
CER	Chevron	

6.0 References

Bartlett, W.L., Friedman, M., and Logan, J.M., 1981, Experimental folding and faulting of rocks under confining pressure, Part IX, wrench faults in limestone layers: Tectonophysics, v. 79, p. 255-277.

Crampin, S., 1990. Alignment of Near Surface Inclusions and Appropriate Crack Geometries for Geothermal Hot-Dry-Rock Experiment. Geophysical Prospecting, v38, p.621-631.

Crampin, S., 1994. The Fracture Criticality of Crustal Rocks. Geophysical Journal International, v. 118, p.428-438.

Crowell, J.C., 1974, Origin of late Cenozoic basins in Southern California: Tectonics and Sedimentation, Soc. Expl. Pal. Min., Spec. Pub. 22, p. 190-204.

Lynn, H.B., 1991. Field Measurements of Azimuthal Anisotropy: First 60m, San Francisco Bay Area, and Estimations of Horizontal Stress Ratios from V_{S1}/V_{S2}. Geophysics, v56, p.822-832.

MacBeth, C., 1995. How Can Anisotropy be Used for Reservoir Characterization? First Break, v13, p.31.

Sales, J.K., 1968, Crustal mechanics of Cordilleran foreland deformation: a regional and scale-model approach: Bull. Am. Assoc. Pet. Geol., v. 52, n. 10, p. 2016-2044.

Sipos, Z. & Marshall, R., 1995. Remarks on Static Corrections for S-Waves. Journal of Seismic Exploration, v.4, p.199.

Sylvester, A.G., and Smith, R.R., 1976, Tectonic transpression and basement-controlled deformation in San Andreas Fault zone, Salton Trough, California: Bull. Am. Assoc. Pet. Geol., v. 68, n. 12, p. 2081-2101.

Tapponnier, P., and Molnar, P., 1976, Slip-line field theory and large scale continental tectonics: Nature, v. 264, p. 319-324.

Tapponnier, P., Peltzer, G., and Armijo, R., 1986, On the mechanics of the collision between India and Asia: *in* Coward, M.P., and Ries, A.C., eds., Collision Tectonics, Geological Society Special Publication n. 19, p. 115-157

Tapponnier, P., Peltzer, G., Le Dain, A.Y., Armijo, R., and Cobbold, P., 1982, Propagating extrusion tectonics in Asia: new insights from simple experiments with plasticine: Geology, v. 10, p. 611-616.

Tapponnier, Peltzer, G., and Armijo, R., 1986, On the mechanics of the collision between India and Asia: the neotectonics of Eastern Anatolia-Young Colision Zone: *in* Coward, M.P., and Ries, A.C., eds., collision tectonics, Geological Society Special Publication n.19, p.115-157.

Tchalenko, J.S., 1970, Similarities between shear zones of different magnitude: Geol. Soc. Am. Bull., v. 81, p. 1625-1640.

Tchalenko, J.S., 1970, Similarities between shear zones of different magnitudes: Bull. Geol. Soc. Am., v. 81, p. 1625-1640.

Tchalenko, J.S., and Ambraseys, N.N., 1970, Structural analysis of Dasht-e-Bayaz earthquake fractures: Geol. Soc. Am. Bull., v. 81, p. 41-60.

Wilcox, R.E., Harding, T.P., and Seely, D.R., 1973, Basic wrench tectonics: Bull. Am. Assoc. Pet. Geol., v. 57, p. 74-96.

Winterstein, D.F. & Meadows, M.A., 1991. Shear Wave Polarizations and Subsurface Stress Directions at Lost Hills Field. Geophysics, v56, p.1349-1364.